Title: Experimental evolution of gene essentiality in bacteria

Authors: Liang Bao[1, *], Zan Zhu[1], Ahmed Ismail[1], Bin Zhu[2], Vysakh Anandan[1], Marvin Whiteley[3], Todd Kitten[1], Ping Xu[1, *]

Affiliations:
1, Department of Oral and Craniofacial Molecular Biology, Philips Institute for Oral Health Research, School of Dentistry, Virginia Commonwealth University, Virginia, USA.
2, Massey Cancer Center, Virginia Commonwealth University, Virginia, USA.
3, School of Biological Sciences, Center for Microbial Dynamics and Infection, Georgia Institute of Technology, Georgia, USA.

Correspondence:

pxu@vcu.edu (P.X.), baol@vcu.edu (L.B.)

Abstract

Essential gene products carry out fundamental cellular activities in interaction with other components. However, the lack of essential gene mutants and appropriate methodologies to link essential gene functions with their partners poses significant challenges. Here, we have generated deletion mutants in 32 genes previously identified as essential, with 23 mutants showing extremely slow growth in the SK36 strain of *Streptococcus sanguinis*. The 23 genes corresponding to these mutants encode components of diverse pathways, are widely conserved among bacteria, and are essential in many other bacterial species. Whole-genome sequencing of 243 independently evolved populations of these mutants has identified >1000 spontaneous suppressor mutations in experimental evolution. Many of these mutations define new gene and pathway relationships, such as F1Fo-ATPase/V1Vo-ATPase/TrkA1-H1 that were demonstrated across multiple *Streptococcus* species. Patterns of spontaneous mutations occurring in essential gene mutants differed from those found in wildtype. While gene duplications occurred rarely and appeared most often at later stages of evolution, substitutions, deletions, and insertions were prevalent in evolved populations. These essential gene deletion mutants and spontaneous mutations fixed in the mutant populations during evolution establish a foundation for understanding gene essentiality and the interaction of essential genes in networks.

Significance

Identifying genes that interact with essential genes offers profound theoretical insights into the basic cellular processes of life and practical benefits for fields such as synthetic biology and the fight against drug resistance. Despite its importance, this task is challenging due to the difficulties in creating essential-gene deletion mutants and linking essential gene functions with their interacting partners. In our study, we changed the transformation system to create viable mutants with deletions in genes previously identified as essential in *Streptococcus sanguinis*.

Fortunately, we obtained dozens of essential gene knockout mutants for the first time. These genes, involved in various pathways, are conserved as core components of the essential genome across many bacterial species. Furthermore, through the experimental evolution of 243 independent populations with deletions in these genes, we identified over 1,000 spontaneous suppressor mutations that affect gene essentiality. This collection of spontaneous suppressor mutations, combined with our essential gene deletion mutants, provides a crucial foundation for elucidating gene essentiality and the interactions of essential genes within cellular networks.

Keywords

Gene essentiality; Experimental evolution; Spontaneous mutations; Whole-genome sequencing; *Streptococcus*; F1Fo-ATPase/V1Vo-ATPase/TrkA1-H1 gene pathway.

Introduction

All living organisms require certain physical properties and biochemical capacities encoded by "essential" genes to sustain basic cellular activities. Essential genes are indispensable for an organism to survive or reproduce, and their essentiality is highly dependent on the environment in which the organism lives. [1-6] *In vivo*, essential gene products carry out these tasks by interacting with other components. Therefore, the essentiality of genes can also depend on the genetic context provided by the additional genes present. [2,7,8] Relationships may be characterized by negative epistasis when the essentiality of a gene is dependent on the absence or impairment of another gene's function, such as synthetic lethality [7,9] or positive epistasis interactions, where an individual with two genes mutated is fitter than a strain possessing a mutant version of only one of the two genes. [7,10,11] In contrast to binary classification, it is increasingly acknowledged that essential genes exhibit a quantitative spectrum, displaying a gradient of essentiality [2,12], and a conditional nature. [13] For some essential genes, under optimal controlled conditions, deletion can still result in viable, albeit severely compromised individuals. [14,15] The loss of essential genes produces intense selective pressure for the fixation of genomic suppressor mutations in the descendants of the original mutants during subsequent generations, including aneuploidy of chromosomes. [14,15] Furthermore, essential genes can lose their essentiality during long-term evolution and acquire novel functions. [16-18] For instance, unlike the essential characteristics of the critical cell cycle regulator *CDK1* in yeasts and animals, [19] plant PSTAIRE-type cyclin-dependent kinases, known as *CDKAs* (plant homologs of *CDK1*), play a role in environmental responses that is independent of the cell cycle, [16] likely after the acquisition of the plant-specific cyclin-dependent kinases, *CDKBs*. [20]

Identifying genes that interact with essential genes can produce many potential benefits, both from a theoretical perspective, such as understanding the basic principles of cellular life,[21,22] and from a practical standpoint, such as addressing various challenges in synthetic biology [23] and combating drug resistance of infectious diseases. [22] Experimental evolution or laboratory evolution imposes a natural selective pressure on a population to redirect the evolution towards fitness-improving phenotypes in a controlled laboratory setting. [14,15,24-30] This methodology has been applied to identify spontaneous mutations associated with fitness-improving phenotypes, such as multicellularity, [24] novel metabolic capacity, [25] restoration of flagellar mobility,[31] and

fitness of minimal cells. [26] Recently, experimental evolution using mutants deleted of essential genes in the yeast *Saccharomyces cerevisiae* revealed a rapid growth phenotype after passages. [14,15] However, aneuploidy of chromosomes was prevalent among evolved populations deleted of essential genes, which hindered the identification of causal suppressors. [14,15] Here, we have established a transformation system to obtain numerous essential gene knockout mutants, including *obgE*, *pfkA*, components of Type-II fatty acid synthesis (FAS II) and subunits of F1Fo-ATPase genes that have been identified as essential in most bacterial species, including all species of *Streptococcus* examined (http://www.essentialgene.org/). Therefore, most of these mutants represent the first of their kind in the entire streptococcal field. For the 23 essential genes whose deletion resulted in a slow-growing phenotype, we performed experimental evolution of their corresponding mutants. After allowing for short-term adaptation, we have identified >1000 spontaneous suppressor mutations in 243 evolved populations deleted of essential genes, most of which are substitutions, deletions, and insertions. This feature enabled us to map virtually all mutations to distinct genomic segments of individual ORFs or intergenic regions. As a proof of concept, we have demonstrated the *f1fo* genes within the F1Fo-ATPase/V1Vo-ATPase/TrkA1-H1 gene pathway across multiple Streptococcus species. For comparison, we also evaluated the twelve mutations that arose in six evolved populations in the wild-type (WT) cells. The mutations that occurred in essential gene mutants displayed several characteristics that distinguished them from those that evolved in WT cells during short-term evolution.

Results

Isolating essential gene mutants and analysis of short-term evolution

The genome of *Streptococcus sanguinis* SK36 comprises over 2000 ORFs, [32] of which 218 have been experimentally identified as essential for the organism's survival when cells are grown on a rich medium—brain heart infusion (BHI) broth or plates—under microaerobic conditions. [1] To isolate viable essential-gene deletion mutants, we have modified our transformation procedure to minimize stress (see Materials and Methods). Although we still employed homologous recombination (Fig. 1a and Supplementary Fig.1a), we replaced our conventional 1-hour aerobic transformation with an anaerobic incubation and a duration of up to 24 hours. [1] Additionally, we optimized the selection conditions by covering the transformants with a thin layer of agar medium and extending the selection period for the transformants to four to six days, all conducted under anaerobic conditions. (See Materials and Methods.)

Using this procedure, we observed an interesting phenomenon. Specifically, for 23 of the essential genes, the transformants produced two types of colonies: large and small (Fig. 1B, and Supplementary Fig.2a). As expected, genotyping of the small colonies revealed a complete replacement of the corresponding ORF with a kanamycin resistance (*kan*) gene (Supplementary Fig.1b). In contrast, genotyping of the large colonies showed that some mutants displayed a "double band" genotype due to duplication of the target gene prior to the replacement of one copy by the *kan* gene (Supplementary Fig.1c, Supplemental Table 1). This finding suggests that *S. sanguinis* SK36 regularly undergoes gene duplications, particularly between two copies of a multi-copy gene or locus, such as the rRNA operons. Alternatively, some large colonies lacked a

130 *kan* gene, but contained point mutations in different genes, with the majority of isolates acquiring
131 mutations in translational machinery genes that may confer resistance to kanamycin, [33] such as
132 *fusA, rpsL* or *rplF* (Supplemental Table 1). Among fifty-four large colonies genotyped, fifteen
133 showed the double-band genotype. The remaining thirty-nine did not contain the *kan* gene, but
134 thirty-eight, or 97.4% contained mutations in *fusA, rpsL* or *rplF* (Supplemental Table 1). In
135 contrast, for nine essential genes, the deletion mutants exhibited robust growth (Supplementary
136 Fig.2b). These nine genes included *nrdE, nrdF, nrdH,* and *nrdI* which were previously reported
137 as non-essential under anaerobic conditions but essential in the presence of O_2, [34] along with
138 *rexB* for ATP-dependent nuclease subunit B, *rpsA* for 30S ribosomal protein S1, *pdf* for peptide
139 deformylase, and *g6pD* for glucose-6-phosphate dehydrogenase (Supplementary Fig.2b).
140
141 We, therefore, directed our attention to the twenty-three essential genes that, when deleted, led to
142 severe growth defects in the resultant mutants. These twenty-three genes encoding components
143 of diverse pathways, include the eight subunit genes encoding the F1Fo-ATPase (*uncE*, *uncB*,
144 *uncF*, *uncH*, *uncA*, *uncG*, *uncD*, and *uncC)*; *ftsX,* encoding a permease-like cell division protein;
145 five *fab* genes (*fabH*, *fabK*, *fabG*, *fabF*, and *fabZ*) that are involved in Type-II fatty acid
146 synthesis (FAS II); two ribosomal protein genes (*rplV* and *rpmH*); two GTPase genes (*obgE* and
147 *yihA*); *yqeG,* encoding a YqeG-family phosphatase; *pfkA*, encoding 6-phosphofructokinase,
148 involved in glycolysis; *pngM*, encoding phosphoglucomutase; *dpcK* (also called *coaE*), encoding
149 diphospho-CoA kinase, involved in CoA synthesis; and *dnaK*, encoding a heat shock protein
150 chaperone. These genes are widely distributed and are essential in various genera and species
151 (http://www.essentialgene.org/). [35] In total, we have created 23 essential gene mutants, each with
152 an individual gene deletion, along with one mutant deleted for the entire *f1fo* region encoding the
153 eight F1Fo-ATPase subunits, which we have named Δ*f1fo* (Supplementary Fig.1 and S2a.1-a.2).
154 Although the deletion mutants of the 23 genes were initially generated under anaerobic
155 conditions in this study, we have confirmed the viability of mutants under both anaerobic
156 (Supplementary Fig.3a) and microaerobic (Supplementary Fig.3b) conditions, as utilized
157 previously for identification of essential genes in *S. sanguinis* SK36. [1] To further verify that the
158 viability of these 24 gene deletion mutants was not due to the absence of oxygen, we randomly
159 selected three essential gene deletions—*pfkA*, *dpcK*, and the entire *f1fo* region—and confirmed
160 that we were able to obtain viable, though extremely slow-growing, target gene deletion mutants
161 under microaerobic conditions as well (data not shown).
162
163 In order to study the evolution of gene essentiality, we conducted passage experiments using
164 multiple independently evolved populations of the 24 essential gene mutants. To form a
165 population, we selected three to five colonies from the selection medium, combined them into a
166 single inoculum, and subjected them to passage in BHI by 1:20 serial transfer. To ensure a
167 comparable number of generations, we closely monitored the growth of mutants during each
168 passage. We proceeded to the following passage only when the cell cultures had reached an
169 OD_{600} within the range of 0.1-0.5. As a control, WT cells, which reached an OD_{600} of
170 approximately 1.0 within 24 hours of growth, or 2-10 times more cells compared to the mutants
171 in each passage, were passaged daily for a total of nine times (Fig. 1c). This method was applied
172 to maintain consistency throughout the experimental process (Fig. 1d, Supplementary Fig.3c, and
173 Supplemental Table 2). While all mutants exhibited significant growth defects compared to WT,
174 we observed variations in their growth phenotypes. Notably, mutants lacking *pfkA, fabK, fabG,*
175 *fabF*, and *fabZ* displayed the most severe growth defects. In contrast, the growth of others,

including another *fab* mutant, *fabH,* was less severe, as evidenced by the OD_{600} measurements of the evolved mutants (Fig. 1c and Supplementary Fig.3c, Supplemental Table 2). In our passage experiments, we observed that the mutants in passage 6 (P6, "P" for passage) exhibited enhanced fitness compared to those in early passages. For example, the time required for cultures to reach an OD_{600} of 0.1-0.5 in P0 compared to P6 (Fig. 1d, Supplemental Table 3) indicated faster growth at P6, reflecting improved fitness.

Identification of suppressor loci in evolved populations deleted of essential genes and in WT

To identify suppressor mutations in the evolved populations deleted of essential genes, we performed whole-genome sequencing at P6 (Fig. 1c). Specifically, we sequenced between two and twenty-five independently evolved populations for each of the twenty-four essential gene mutants, resulting in a total of 243 populations (Fig. 2a and Supplemental Table 4). As controls, we also sequenced six populations of WT, which were generated by aliquoting into six separate tubes and passaging nine times, as well as the original WT (Fig. 2a and Supplemental Table 4).

We first considered mutations related to duplications of genes other than the essential gene targeted for mutagenesis. Of the 243 evolved mutant populations, we found that twelve (4.9%) displayed gene duplications of various sizes, ranging from 10 kb to 310 kb. By comparison, none of the six evolved WT populations in P9 nor the original parental WT contained a gene duplication (Supplementary Fig.4a). For the twelve evolved mutant populations with gene duplications, two were from Δ*f1fo* (*#107* and *#109*) (Fig. 2a and Supplementary Fig.4b), one from Δ*uncE* (*#2*) (Supplementary Fig.4c), one from Δ*uncH* (*#7*) (Fig. 2c), three from Δ*fabH* (#4, #6 and #14) (Fig. 2d and Supplementary Fig.4d and S4e), one from Δ*fabF (#4)* (Fig. 2e), two from Δ*fabZ* (*#1 and #3*) (Fig. 2f and 2c), one from Δ*obgE* (*#5*) (Fig. 2h) and one from Δ*dpcK* (*#17*) (Fig. 2i). The duplicated regions found in populations of Δ*f1fo,* Δ*uncE,* Δ*uncH,* Δ*fabH* and Δ*fabF* mutants encompassed the same ~103 kb region (coordinate: 22,738-125,834) that is flanked by two directly repeated rRNA operons (Fig. 2b-e). The above-duplicated region of ~103 kb contains 113 ORFs, including nine ORFs encoding the entire V1Vo-ATPase operon that is related to the proton pump function of F1Fo-ATPase, [36] one ORF encoding acyl carrier protein and one ORF encoding acyltransferase that is related to lipid biosynthesis. [37] The duplicated region found in Δ*fabZ#1* spans approximately 143 kb (coordinate: 1,053,488-1,197,391). The 10.1-kb duplication in Δ*fabZ#3* (coordinate: 1,093,824-1,103,958) is within the duplicated 143 kb in Δ*fabZ#1.* This 10.1-kb region contains ten ORFs, including one ORF annotated as acyl-acyl carrier protein thioesterase, which catalyzes the terminal reaction of fatty acid biosynthesis (Jing, et al., 2011). In the case of Δ*obgE#5*, a 37-kb duplication is present (coordinate: 1,775,394-1,812,805), encompassing thirty ORFs, including one ORF encoding der GTPase. In Δ*dpcK#17,* a ~310-kb duplication occurred (coordinate: 385,678-697,581), encompassing 305 ORFs. The flanking sequences of the duplicated regions in Δ*fabZ#1,* Δ*fabZ#3,* Δ*obgE#5* and Δ*dpcK#17* possessed no notable repeated sequences.

Next, we assessed substitutions, deletions, and insertions of less than 10 kb in the evolved populations. The genome of *S. sanguinis* can be divided into 4,283 segments—2,340 ORFs and 1,943 intergenic regions (Supplemental Table 5). [38] We defined a segment as mutated if any mutation within that segment was present in at least 30% of the sequence reads (see Materials

222 and Methods section). We selected 30% as the threshold based on our finding that confirmed
223 suppressor mutations, such as *trkA1-H1*, ranged from 34.8% to 100% in the evolved Δ*f1fo*
224 populations in P6 (Fig. 4d and Supplemental Table 4). There were six mutations (two
225 substitution mutations and four deletion mutations from the six evolved populations), where two
226 to four ORFs were affected by each mutation. For example, the C to T (at coordinate 1,313,563)
227 mutation in Δ*fabF#10* caused amino substitutions of two overlapping ORFs encoding two
228 hypothetical proteins (Supplemental Table 4). The remaining mutations fell within single
229 segments of ORFs or intergenic regions. In total, we detected 1,272 mutated segments
230 (Supplemental Table 4), with 1,260 from evolved populations lacking essential genes and twelve
231 from the evolved WT populations (Supplemental Table 4). Our analysis revealed that each of the
232 243 (100%) evolved mutant populations contained at least one mutated segment, with the
233 majority containing from 2 to 10 (Fig. 2j and Supplemental Table 4-6). In contrast, among the
234 six evolved WT populations, four had at least one segment containing a mutation in at least 30%
235 of the sequence reads, while the remaining two, as well as the parental WT population, had none
236 (Fig. 2j and Supplemental Table 4). Furthermore, when we set the threshold to 50%, 241 evolved
237 mutant populations, or 99.2%, had mutated segments, whereas none of the six evolved WT
238 populations contained mutated segments (Fig. 2k and Supplemental Table 7) ($\chi2$=154.69, df=1,
239 n=249 populations, p=2.2e-16).
240
241 We then analyzed the presence of mutated segments belonging to essential ORFs (in each case,
242 excluding the ORF that was intentionally deleted in each mutant, as well as the nine
243 conditionally essential genes). We found that suppressor mutations belonging to essential
244 segments were present in at least one evolved population from each essential gene mutant (Fig.
245 2l and Supplemental Table 8-9). In contrast, none of the twelve mutated segments from the
246 evolved WT populations were found to be within an essential ORF (Fig. 2l and Supplemental
247 Table 8-9) ($\chi2$=5.74, df=1, n=25 groups, p=0.017). To illustrate this further, we compared the
248 frequency of mutated segments in P1 and P6 for two specific cases: mutations of *ftsZ* (an
249 essential segment encoding a structural homolog of tubulin in prokaryotes) in the evolved
250 Δ*f1fo#107* and *uncH* (an essential segment, encoding delta subunit of F1Fo-ATPase) in the
251 evolved Δ*uncC#1*. The *uncH* gene is located 3.9 kb upstream of *uncC*, both of which are within
252 the *f1fo* operon. The evolved Δ*uncC#1* population of P1 did not have any *uncH* mutations using
253 30% as the cutoff, although an *uncH* mutation was present in 12% of the sequence reads
254 (Supplementary Fig.5a-c). In contrast, the Δ*uncC#1* population of P6 contained 86% *uncH*
255 mutation (Supplementary Fig.5d-f) The resultant mutation replaced a 207-bp segment that was
256 51 bp downstream of the *uncH* start codon with an 82-bp fragment, causing early truncation
257 (Supplementary Fig.5g). For the second case, the *ftsZ* gene is located approximately 126 kb
258 upstream of the *f1fo* operon. In the evolved Δ*f1fo#107* population in P1, we did not detect any
259 mutations in the *ftsZ* segment using 30% abundance as cutoff, although 27% of the sequence
260 reads contained a *ftsZ* mutation (Supplementary Fig.5g-h). In comparison, the evolved
261 population of P6 contained 100% mutated *ftsZ*—a 248 bp insertion located 1015 bp downstream
262 of the start codon (Supplementary Fig.5I-J), leading to the truncation of the FtsZ protein
263 (Supplementary Fig.5k). These findings demonstrate an increase of mutated essential segments
264 in the essential gene deletion mutant due to selection during passage.
265
266 Multi-drug resistance across ESKAPE pathogens (i.e., *Enterococcus faecium*, *Staphylococcus*
267 *aureus*, *Klebsiella pneumoniae*, *Acinetobacter baumannii*, *Pseudomonas aeruginosa*, and

268 *Enterobacter spp.*) has been found to be commonly associated with mutations in six genes—
269 namely, *rrs, gyrA*, *gyrB*, *rpoB, rpsL* and *rsmG* (also known as *gidB*). [39] We therefore asked
270 whether mutations in the typical set of multi-drug resistance-associated genes [39] could appear in
271 the evolved populations deleted of essential genes. Apart from the 16S rRNA gene, which is
272 present in four copies (*rrs1* to *rrs4*), *S. sanguinis* has one copy of each of these genes. Among
273 the 243 evolved populations deleted of essential genes, mutations of multi-drug resistance genes
274 were present in *rrs2*, *rpoB*, *gyrB,* and *rspL* in a variety of populations derived from different
275 essential gene mutants, while no mutations were detected in *rrs1*, *rrs3*, *rrs4*, *gyrA* or *rsmG*.
276 Moreover, no mutation was detected within this set of multi-drug resistance-associated genes in
277 the evolved WT populations (Fig. 2m and Supplemental Table 10). These results showed that
278 missense mutations in four of the same genes that promote multi-drug resistance also improve
279 the fitness of mutants deleted of these particular essential genes.
280
281 In summary, compared to the evolved WT populations, mutants deleted for essential genes
282 exclusively evolve gene duplications of greater than 10 kb, mutations in essential genes, and
283 mutations of genes associated with multi-drug resistance. In addition, once mutations are
284 observed, they are more quickly fixed in the population (Fig. 2k).
285
286 **Construction of a network using WT and essential gene deletion mutants and their**
287 **suppressors**
288
289 To explore the relationships of suppressor mutations from the evolved populations, we
290 established a network of 25 groups, comprising the 24 mutants deleted for essential genes, along
291 with SK36, and their respective evolved suppressors across 249 populations (243 populations
292 from mutants and six populations from SK36). In these 249 populations, 1,272 mutations
293 occurred in 592 distinct segments, with 503 segments belonging to ORFs and 89 belonging to
294 intergenic regions (Fig. 3a, Supplemental Table 4, and Supplemental Table 11-13). This network
295 also encompasses a total of 914 edges connecting these 617 nodes (Fig. 3a and Supplemental
296 Table 11-13).
297
298 Some mutations discovered in the evolved WT also appeared in evolved mutant populations. The
299 twelve mutations occurred in ten distinctive segments, with 5 segments specific to WT and 5
300 shared with populations derived from essential gene mutants. Notably, the ORF J1C87_09360,
301 annotated as PTS mannose/fructose/sorbose transporter family subunit IID, exhibited mutations
302 in two of the six evolved WT populations. This result is consistent with a previous study in
303 SK36, where fitness improvement was associated with mutations in three ORFs of the same
304 operon (J1C87_09355, J1C87_09360, and J1C87_09365). [40] In the current study, mutations in
305 the three OFRs were also observed in mutant populations of Δ*uncH,* Δ*fabG,* Δ*fabK,* Δ*fabF,*
306 Δ*fabZ, and* Δ*pfkA* (Supplementary Fig.6a-b and Supplemental Table 14). Interestingly, most of
307 the evolved populations that contain suppressor mutations in the three PTS
308 mannose/fructose/sorbose transporter subunits are also those that showed the most severe growth
309 defects, such as Δ*fabG,* Δ*fabK,* Δ*fabF,* Δ*fabZ, and* Δ*pfkA* (Fig. 1d and Supplementary Fig.3c).
310 These results demonstrate that mutations in some segments that apparently improved fitness in
311 WT could also contribute to the fitness improvement of essential gene mutants.
312

313 Mutations in some segments that were present in evolved populations deleted of one essential
314 gene also appeared in evolved populations of other mutants deleted of another essential gene. For
315 example, most populations of the mutant deleted for the entire *f1fo* region (*Δf1fo*) and the eight
316 F1Fo subunits deletion mutants (Δ*uncE,* Δ*uncB,* Δ*uncF,* Δ*uncH,* Δ*uncA,* Δ*uncG,* Δ*uncD* and
317 Δ*uncC)* contain suppressor mutations in J1C87_08610 (*trkA1*) and J1C87_08615 (*trkH1*) (Fig.
318 3a). Mutations in many F1Fo subunits are shared among the evolved populations of various other
319 subunit deletion mutants (Fig. 3a and Supplemental Table 4). Furthermore, many of the
320 suppressor mutations in type II fatty acid synthesis (FAS II) gene mutants, such as Δ*fabZ,* Δ*fabF,*
321 Δ*fabG,* Δ*fabK* and Δ*fabH* and those in the CoA biosynthesis mutant Δ*dpcK*, occur in the same
322 ORFs related to fatty acid biosynthesis, including essential genes like acetyl-CoA carboxylase
323 carboxyl transferase subunit alpha (J1C87_09410: *accA*) and acetyl-CoA carboxylase biotin
324 carboxylase subunit (J1C87_09420: *accC*) (Fig. 3a). Similarly, the suppressors identified in the
325 populations of two ribosomal protein mutants *(*Δ*rpmH* and Δ*rplV*) and two GTPase mutants
326 (Δ*yihA* and Δ*obgE*) include mutations in 50S ribosomal protein gene *rplB* (J1C87_00620) and
327 RNA biosynthesis genes, such as *rpoB* (J1C87_01040) (Fig. 3a and Supplemental Table 4).
328 These findings indicate that mutated segments shared across multiple evolved mutants can confer
329 fitness benefits to mutants deleted of different essential genes.
330
331 We also observed mutual suppressors, where an evolved population deleted of the first essential
332 ORF contained a mutated segment within a second essential ORF, while an evolved population
333 deleted of the second essential ORF contained a mutated segment within the first essential ORF.
334 For example, in the *obgE* deletion mutant *(*Δ*obgE*), a mutation in *dnaK* occurred (Fig. 3a and
335 Supplemental Table 4); conversely, in Δ*dnaK*, a mutated segment of *obgE* was detected (Fig. 3a
336 and Supplemental Table 4). Similarly, in the F1Fo subunit deletion mutant Δ*uncF*, a mutation of
337 *dpcK* was also present (Fig. 3a and Supplemental Table 4). In Δ*dpcK*, mutated segments were
338 detected within *uncA* and *uncD* (Fig. 3a and Supplemental Table 4). Other mutual suppressor
339 pairs include those between subunits of F1Fo (Fig. 3a and Supplemental Table 4) and between
340 components of the FASII system (Fig. 3a and Supplemental Table 4). These results suggest the
341 presence of positive epistasis interactions between different essential gene(s), where strains
342 containing mutations in both essential genes are fitter than those containing mutations in either of
343 the essential genes.
344
345 **Possible explanations for parallel suppressor evolution in mutants deleted for particular**
346 **essential genes**
347
348 Given the potential role of parallel evolution for fitness improvement,[41-43] we next sought to
349 identify the most commonly mutated segments for each essential gene mutant and those
350 clustered in a particular operon. Utilizing these highly occurring suppressors (Supplemental
351 Table 4 and Supplemental Table 16), along with candidate genes within duplicated regions (Fig.
352 2b-h), we aimed to elucidate the mechanisms by which they improved the growth of mutants
353 deleted for essential genes.
354
355 <u>Δ*f1fo suppressors*</u>
356 F1Fo is proposed to function as an ATP-dependent proton pump in streptococci, including *S.*
357 *mutans* and *S. sanguinis*.[44] Mutations in *trkA1* or *trkH1* are present in all thirteen evolved
358 populations of Δ*f1fo*, with twelve populations containing *trkH1* mutations and one containing a

359 *trkA1* mutation (Fig. 3b and Supplementary Fig.7, Supplemental Table 4 and Supplemental
360 Table 16). Similarly, mutations in *trkA1*, *trkH1*, or a one base pair (bp) insertion mutation
361 located 38 bp upstream of the *trkA1-H1* operon (P_trkA1-H1, "P" for promoter) are found in
362 twenty-five out of twenty-six (96.2%) of the evolved populations deleted of single F1Fo subunits
363 (Fig. 3b and Supplementary Fig.7, Supplemental Table 4 and Supplemental Table 16). Among
364 the twenty-three mutations in the ORFs of *trkA1-H1*, sixteen populations have *trkH1* mutations,
365 and eight have *trkA1* mutations. Given the comparable length of *trkA1* (1350 bp) and *trkH1*
366 (1440 bp), it appears that mutations in the *trkH1* gene are more likely than mutations in *trkA1* to
367 improve the fitness of mutants deleted for F_1F_o subunits.
368
369 We also observed that gene duplications occurred in the same region across populations deleted
370 of all F1Fo subunits or single subunits, i.e., Δ*f1fo#107* and *#109* (Fig. 2b and Supplementary
371 Fig.4b), Δ*uncE#2* (Supplementary Fig.4c) and Δ*uncH#7* (Fig. 2c). This region of approximately
372 103 kb (coordinates: 22,738-125,834) contains the *v1vo* operon encoding the V1Vo-ATPase,
373 which has been proposed to function as a proton pump [36] and may compensate for the loss of
374 *f1fo*. It is interesting to note that Δ*uncH#7* is the only evolved population listed above that lacks
375 mutations in the flanking upstream regions or the ORFs of *trkA1* or *trkH1* (Fig. 2c). More
376 interestingly, among the evolved populations deleted of F_1F_o subunits (thirteen Δ*f1fo* and twenty-
377 six mutants deleted for single *unc* subunit genes), Δ*uncE#2* and Δ*uncH#7* are the only two
378 populations that contain amino acid substitution mutations of V-type ATP synthase subunits
379 (Supplemental Table 4 and Supplemental Table 16).
380
381 Suppressor mutations appeared in other F1Fo subunits or intergenic regions of *f1fo* in many
382 evolved populations deleted of a single subunit (Fig. 3b and Supplementary Fig.7). This result
383 suggests that for the F_1F_o complex, when one subunit is absent, other subunits cannot function
384 properly and their presence is detrimental to the mutant.
385
386 Given that V1Vo may also function as an ATP-dependent proton pump [36] and the Trk system
387 works as a symporter (K+/Na+ or K+/H+), [45] we hypothesize that *v1vo* can partially compensate
388 for the loss of *f1fo*, that TrkA1-H1 is the major contributor to acidification of the cytosol when
389 pumping in K+, and that the function of TrkA1-H1 must therefore be inhibited when F1Fo is not
390 present (Supplementary Fig.11).
391
392 *ΔftsX suppressors*
393 FtsEX is crucial in regulating divisome assembly and activation at the plasma membrane and cell
394 wall. [46] In the evolved *ΔftsX* populations, mutations in the *ftsE* gene of the *ftsEX* operon and the
395 *vicRK (vicK/walK* and *vicR/walR)* two-component system (TCS) frequently occurred (Fig. 3b
396 and Supplementary Fig.7). Mutations in *ftsE* were present in eight out of nineteen evolved *ΔftsX*
397 populations (42.1%); in one of these populations, *ΔftsX#13*, a deletion mutation at 51 bp of the
398 693 bp *ftsE* ORF leads to a frameshift in the N-terminal region (Fig. 3b and Supplementary
399 Fig.7). This observation suggests that in the absence of *ftsX*, *ftsE* does not function properly and
400 is deleterious to the cell. Although *vicR* and *vicK* compose a TCS, *vicK* is not essential, while
401 *vicR* is essential. [1,47] Fifteen populations contained *vicK* mutations (with one frameshift and one
402 truncation), and one population contained a *vicR* mutation (an amino acid substitution, M54V),
403 collectively representing 89.5% of the evolved populations (Fig. 3b and Supplementary Fig.7,
404 Supplemental Table 4 and Supplemental Table 16). It was reported that FtsEX interacts with the

405 cell wall component peptidoglycan hydrolase, PcsB, which is positively regulated by the
406 *vicRK/walRK* two-component regulatory system. [48] Therefore, we hypothesize that when FtsEX
407 is absent and PcsB cannot function properly, there is a need to inhibit the activity of PcsB's
408 upstream regulatory factor, VicRK.
409
410 *fab operon suppressors*
411 The *fabH, fabF, fabG, fabZ, and fabK* genes belong to a FASII operon containing thirteen ORFs
412 in total, with a MarR family transcriptional regulator gene (*fabT*) upstream and seven other
413 genes. In the evolved populations of Δ*fabZ,* Δ*fabF,* Δ*fabG,* Δ*fabK,* and Δ*fabH*, we observed a
414 significant enrichment of mutations in genes encoding components of the FASII system (Fig. 3b
415 and Supplementary Fig.7, Supplemental Table 4, and Supplemental Table 16). This result
416 suggests that when one component of the FASII system is deleted, this can trigger genome
417 changes in other FASII components, leading to fitness improvement.
418
419 There is a notable number of populations containing a duplication of approximately 103 kb
420 (coordinate: 22,738-125,834) in the Δ*fabH,* Δ*fabF,* and Δ*fabG* mutants, which includes one ORF
421 encoding an acyltransferase and one ORF encoding acyl carrier protein. Additionally, a
422 duplicated region of 10.1 kb (coordinate: 1,093,824-1,103,958) is shared by Δ*fabZ #1* and Δ*fabZ*
423 *#3* and contains acyl-acyl carrier protein thioesterase. We hypothesize that these duplications
424 may enhance fatty acid synthesis when *fabK, fabZ, fabH, fabF, or fabG* is defective.
425
426 Δ*dpcK suppressors*
427 DPCK is the final enzyme in the five-step pathway for CoA biosynthesis. [49] In the evolved
428 Δ*dpcK* populations*,* mutations ≤100 bp upstream of *acpS* (encoding holo-ACP synthase) are
429 present in eleven of the seventeen Δ*dpcK* populations. Holo-ACP synthase, responsible for
430 covalent attachment of CoA to acyl carrier protein, uses CoA as a substrate for fatty acid
431 biosynthesis. [50] Among the seventeen populations, one population, Δ*dpcK#17,* contained a gene
432 duplication; we were not able to identify the gene(s) responsible for improved growth due to the
433 large size of the duplication (>300 kb, containing 305 ORFs; Fig. 2i). We hypothesize that holo-
434 ACP synthase is a significant contributor to the use of CoA, and when there is a shortage of
435 CoA, fatty acid production needs to be reduced by lessening the expression of *acpS* (Fig. 3b and
436 Supplementary Fig.7, Supplemental Table 4 and Supplemental Table 15). Consistent with the
437 fitness improvement of Δ*dpcK* by reducing CoA usage, seven out of the seventeen Δ*dpcK*
438 populations contain mutations in the FASII operon (Fig. 3b and Supplementary Fig.7;
439 Supplemental Table 15).
440
441 Δ*pfkA suppressors*
442 *pfkA* encodes 6-phosphofructokinase (PFK), responsible for catalyzing the phosphorylation of
443 fructose-6-phosphate to fructose-1,6-bisphosphate, a committing step in glycolysis. [51] In the
444 evolved Δ*pfkA* populations, we observed an enrichment of mutations in *fruR, fruB,* and *glck*.
445 Among the ten Δ*pfkA* evolved populations (Fig. 3b and Supplementary Fig.7; Supplemental
446 Table 4, and Supplemental Table 15), six populations contained mutations in *fruR*, five
447 populations had mutations in *fruB*, and nine populations had mutations in *glcK*. The *glcK* gene
448 encodes an ROK domain-containing glucokinase, which phosphorylates glucose to produce
449 glucose-6-phosphate, a progenitor of fructose-6-phosphate. [52] The *fruR* gene encodes a
450 transcriptional repressor of the *fruBA* operon, while *fruB* (also known as *pfkB*) has been

451 demonstrated to function as a 1-phosphofructokinase in multiple bacterial species, [53] including
452 streptococci. [54] Interestingly, the nature of the mutations differed according to the gene; three of
453 the eleven *glcK* mutations were truncations, and four of the seven *fruR* mutations were
454 truncations or frameshift mutations, while none of the seven *fruB* mutations were truncations or
455 frameshifts (Supplemental Table 4 and Supplemental Table 15).
456
457 We hypothesize that in the absence of *pfkA*, accumulated fructose-6-phosphate becomes toxic, as
458 has been shown previously in other bacterial species. [53] Elimination of GlcK activity would
459 reduce fructose-6-phosphate production. We further hypothesize that FruB possesses low levels
460 of fructose-6-phosphate kinase activity, thus replacing PfkA, but only when the expression of
461 *fruB* is increased due to *fruR* mutation or the fructose-6-phosphate kinase activity of FruB is
462 increased due to alteration of its sequence. This mechanism would be similar to findings in *E.*
463 *coli*, where a mutation that increased *fruB* expression was found to suppress the phenotype of
464 Δ*pfkA* mutants. [55,56]
465
466 <u>Δ*obgE suppressors*</u>
467 ObgE belongs to the TRAFAC (Translation Factor Association) class of P-loop GTPases, which
468 is highly conserved and essential in bacteria. [57] The ObgE GTPase is known to play a wide range
469 of functions, with some of the most significant roles including sporulation initiation in *Bacillus*
470 *subtilis*, [58] aerial mycelium formation in *Streptomyces*, [59,60] bacterial persistence in *E. coli* and
471 *Pseudomonas aeruginosa*, [61] involvement in ribosome biogenesis, [62,63] participation in DNA
472 replication, [64-66] and contributions to chromosome segregation and cell division. [67]
473
474 Among the fourteen evolved Δ*obgE* populations, eight populations had substitution mutations
475 upstream of *rpoB* (seven were an A to T mutation 321 bp upstream of the start codon, and the
476 other was an A to G mutation 24 bp upstream), and two populations contained substitution
477 mutations within the *rpoB* ORF (one at 905 bp and the other at 1058 bp from the start of the
478 3567 bp ORF). In total, 71.4% of the populations had mutations within or upstream of *rpoB* (Fig.
479 3b and Supplementary Fig.7; Supplemental Table 4 and Supplemental Table 15). The *rpoB* gene
480 codes for the beta-subunit of RNA polymerase I. In one of these populations, Δ*obgE#5*, a 37 kb
481 gene duplication was observed (coordinate: 1,775,394-1,812,805), encompassing thirty ORFs,
482 including one annotated as Der GTPase. It was reported that overexpression of *der* or *obgE* can
483 suppress growth defects of a mutant lacking *rrmJ* that encodes the methyltransferase for U2552
484 of the 23S rRNA. [68] From this, we hypothesize that the duplication may partially compensate for
485 the loss of ObgE function by increasing *der* copy numbers, and a reduction in RNA synthesis is a
486 significant fitness adaptation when ObgE is defective.
487
488 <u>*WT and other mutant suppressors*</u>
489 Suppressor mutations in the evolved populations of Δ*pngM*, Δ*yqeG,* Δ*dnaK,* Δ*yihA,* Δ*rpmH,*
490 Δ*rplV,* and WT are less easily explained, and further study is required to identify possible
491 mechanisms (Supplementary Fig.7 and Supplemental Table 15).
492
493 **Testing the working model involving *f1fo, v1vo, trkA1-H1* and *trkA2-H2***
494

To test the hypotheses proposed above, we have chosen F1Fo-ATPase, an evolutionarily ancient enzyme complex that is highly conserved across virtually all forms of cellular life [69] and has been reported as essential for entire genus of the streptococcal species. [35]

We began by testing whether increasing copy numbers of *v1vo* contributes to the fitness improvement of the mutant deleted for the entire F1Fo complex or single subunits. To explore this, we examined the gene duplication of the *v1vo* region at the early stage, P1 in the four populations that contain gene duplications at P6 (Fig. 2b-c, Supplementary Fig.4b-c, and Supplementary Fig.8a). Among these four populations, one had the gene duplication at P1, while the other three acquired the duplication during subsequent passages (Figure 4a and Supplementary Fig.8a). This observation indicates that gene duplications of the *v1vo* region evolved in these populations after initial passages.

To further confirm the increased fitness of *v1vo* region duplications in populations lacking *f1fo*, we subcultured five *Δf1fo#4* populations from the P6 stage, which did not initially contain gene duplications in the *v1vo* region. After nine additional passages (P15), we observed that two out of the five evolved populations had *v1vo* region duplications in P15 (Fig. 4b and Supplementary Fig.8a).

To ascertain the fitness improvement by increasing *v1vo* copy numbers in mutants lacking *f1fo*, we tested whether *v1vo* could be deleted in *Δf1fo*. We first deleted the entire *v1vo*, which consists of nine subunits, to generate the *Δv1vo* mutant in the WT background. This *Δv1vo* mutant grew indistinguishably from the wild type in a rich medium (data not shown), demonstrating that *v1vo* can be deleted when *f1fo* is intact (Fig. 4c). However, when we attempted to delete *v1vo* in *Δf1fo#4*, where *f1fo* was removed, it resulted in a double-band genotype in all five *Δv1vo-DB/Δf1fo#4* ("DB" for double-band) lines tested (Fig. 4c and Supplementary Fig.9). Consistent with these findings, Δ*uncE#2* and Δ*uncH#7*, which contain amino acid substitution mutations of V1Vo ATP synthase subunit A and K in the *v1vo* operon, respectively, also contain *v1vo* region duplications (Supplemental Table 4). This finding indicates that increased copy numbers of the *v1vo* genes compensated for the loss of F1Fo function. Overall, these results suggest that increasing the copy numbers of *v1vo* contributes to the fitness improvement of mutants lacking *f1fo*.

We then investigated the impact of inhibiting *trkA1-H1* on enhancing the fitness of *Δf1fo*. Initially, we compared the occurrence of *trkA1-H1* mutations between P1 and P6 stages across twelve independently evolved populations of *Δf1fo* (*#101* to *#112*). While mutations in the *trkA1* or *trkH1* segments were not detected in P1 using a 30% threshold in nine of the twelve populations, we observed *trkA1-H1* mutations in all populations, with the mutation frequency increasing during passage in all six independently evolved populations (Fig. 4d and Table S17). These mutations resulted in at least one frameshift and various substitutions in the translation of TrkA1 or TrkH1 in six populations, while in the remaining populations, they led to a histidine insertion or various substitutions in the TrkH1 protein (Supplemental Table 16). This data indicates the fixation of *trkA1-H1* mutations during passage.

To further investigate the impact of *trkA1-H1*, we compared the growth of *Δf1fo* in the presence and absence of *trkA1-H1*. *S. sanguinis* SK36 has two Trk systems, *trkA1-H1* and *trkA2-H2*. The

541 growth of *trkH2*, or double-gene deletion mutants of *trkA1-H1* or *trkA2-H2,* were
542 indistinguishable from that of WT (Fig. 4e, Supplementary Fig.10a-f and Supplemental Table
543 17). However, combined deletion of either *trkA1* or *trkH1* along with *trkH2* resulted in growth
544 defects (Fig. 5e-g, Supplementary Fig.10g-h, and Supplemental Table 17), indicating that *trkA1-*
545 *H1* and *trkA2-H2* are redundant for growth. In order to determine the effect of mutating the two
546 Trk systems on the fitness of *Δf1fo*, we transformed the *Δf1fo* construct into the backgrounds of
547 *ΔtrkA1-H1*or *ΔtrkA2-H2*, and compared the growth of the *Δf1fo/ ΔtrkA1-H1* mutant and that of
548 *Δf1fo/ΔtrkA2-H2*. As controls, we also included *Δf1fo#4*, which contains a frameshift mutation of
549 *ΔtrkH1* in the *Δf1fo* background (Supplemental Table 4). It showed that while the growth of
550 *Δf1fo#4* and *Δf1fo/ΔtrkA1-H1* were comparable to each other, the growth of *Δf1fo/ΔtrkA2-H2*
551 was significantly inhibited compared to that of *Δf1fo#4* and *Δf1fo/ΔtrkA1-H1.* (Fig. 4f-g and
552 Supplemental Table18). These findings suggest that inhibiting *trkA1-H1*, but not *trkA2-H2*,
553 contributes to the fitness improvement of evolved mutants deleted for *f1fo*.
554
555 In lactic acid bacteria, F1Fo-ATPase is believed to function by pumping out protons to alkalinize
556 the cytosol or to build negative internal and positive external membrane potentials. [70] To test
557 whether the growth defects in the *S. sanguinis Δf1fo* mutant are due to impaired function in
558 alkalinizing the cytosol or building a membrane potential, we compared the growth of *Δf1fo#4* in
559 a rich medium supplemented with lactic acid (which increases membrane potential and cytosolic
560 proton concentration) or NaOH (which lowers membrane potential and cytosolic proton
561 concentration). We observed that *Δf1fo#4* is susceptible to lactic acid treatment compared to WT
562 (Fig. 4h and Supplemental Table 18). Conversely, the growth defect of *Δf1fo#4* can be partially
563 rescued by NaOH within a certain range (Fig. 4i and Supplemental Table 18). These results
564 suggest that *f1fo* in *S. sanguinis* functions by pumping out protons to alkalinize the cytosol.
565
566 We therefore suggest the following model for the relationship of *f1fo* with *v1vo, trkA1-H1,* and
567 *trkA2-H2* (Supplementary Fig.11). For streptococci, which do not contain the tricarboxylic acid
568 cycle or electron transport chain, energy production is mainly through lactic acid fermentation. [71]
569 The lactate from fermentation creates highly acidic cytosol, which would be toxic if H+ were not
570 exported. F1Fo pumps out H+ from the cytosol using ATP. Both TrkA1-H1 and TrkA2-H2 are
571 potassium transporters and functionally redundant for that purpose. TrkA1-H1 pumps in
572 potassium together with H+, acidifying the cytosol when H+ is not exported. In contrast, TrkA2-
573 H2 does not pump protons into the cytosol when pumping in potassium (likely instead pumping
574 in Na+). Therefore, the function of TrkA1-H1 must be inhibited if F1Fo is not functional.
575
576 **Conserved functional relationships of *f1fo*, *trkA1-H1, trkA2-H2* and *v1vo* in different**
577 **streptococci**
578
579 To generalize the *f1fo* working model and assess F1Fo's essentiality in other strains and species,
580 we conducted essentiality evaluations in three other streptococci: *S. mutans* UA159, *S. sanguinis*
581 SK405, and *S. sanguinis* SK1058. Genomic sequencing of *S. mutans* UA159, [72] *S. sanguinis*
582 SK405 [38,] and *S. sanguinis* SK1058 [38] showed that *f1fo* and *trkA1-H1* are present in all three
583 strains, as in SK36, while *v1vo* is present in the *S. sanguinis* strains only. *TrkA2-H2* is present in
584 both *S. sanguinis* SK36 and SK405 but not in *S. sanguinis* SK1058 or *S. mutans* UA159 (Fig.
585 5a).
586

587 To assess whether *v1vo* could serve as a partial backup in cases of F1Fo loss-of-function, we
588 attempted to delete *f1fo* in *S. mutans* UA159, which lacks *v1vo*. Despite multiple attempts and a
589 total of 64 independent genotyping analyses, none of the transformants were deleted for *f1fo*,
590 instead producing a double band indicative of gene duplication prior to allelic exchange
591 (Supplementary Fig.12a-b). This result highlights that in *S. mutans* UA159, lacking *v1vo, f1fo*
592 cannot be deleted in our conditions. This observation supports the evolutionarily conserved
593 relationship between *f1fo* and *v1vo* observed in other streptococcal species.
594
595 We then investigated the impact of deleting *trkA1-H1* in the other two strains: *S. sanguinis*
596 SK1058, which only possesses *trkA1-H1*, and *S. sanguinis* SK405, which has both *trkA1-H1* and
597 *trkA2-H2*. Our findings showed that *trkA1-H1* mutants exhibited severe growth defects in the
598 SK1058 background compared to the SK405 background (Fig. 5d-e; Supplementary Fig.13a-c).
599 This result demonstrates the requirements of the *Trk* system for growth within the species of *S.*
600 *sanguinis*.
601
602 Next, we investigated the possibility of deleting *f1fo* in *S. sanguinis* SK1058 and SK405, both of
603 which contain *v1vo* and *trkA1-H1*. We could generate *f1fo* whole-region deletion mutants (*Δf1fo*)
604 in both SK1058 and SK405 backgrounds (Fig. 5b, 5c, Supplementary Fig.14). Furthermore, the
605 growth of mutants with *f1fo* deletions in SK405 was notably better than in SK1058 (Fig. 5b, 5d-
606 f; Supplemental Table 19). To explore the potential emergence of *trkA1-H1* suppressor mutations
607 during evolution, we conducted passage experiments using independently evolved populations
608 with *f1fo* deletions in SK405 (Supplementary Fig.14a: three populations) and in SK1058
609 (Supplementary Fig.14b: two populations). It was observed that, after six passages, *trkA1-H1*
610 suppressor mutations appeared in all evolved *Δf1fo* populations in SK405 and SK1058 (Fig. 5e).
611 At least one population each in the SK405 and SK1058 backgrounds are frameshift or truncation
612 mutations of *trkA1-H1* (Fig. 5g and Supplemental Table 20). This result underscores the
613 evolutionarily conserved occurrence of *trkA1-H1* suppressor mutations in evolved populations
614 with *f1fo* deletions.
615
616 **Discussion**
617
618 While identifying genes that interact with essential genes or compensate for their loss provides a
619 great benefit, [4] this task remains challenging, primarily due to the unavailability of essential-gene
620 deletion mutants and systematic methodologies to connect the function of essential genes with
621 their partners. Traditional approaches, such as conditional promoter-shutoff[73,74], antisense RNA
622 knockdowns [48] and CRISPR interference, [75,76] while valuable, may exhibit limitations, including
623 incomplete target gene silencing and suboptimal design efficacy, [76] thereby potentially
624 compromising the reliability of essential gene functional analyses. Our study successfully
625 established a system to generate viable mutants with deletions in essential genes (Fig. 1 and
626 Supplementary Fig.1-S2). We observed that small colonies likely represent the deletion mutants,
627 while large colonies often exhibit the "double-band" genotype or kanamycin resistance due to
628 mutations in translational machinery.
629
630 With these observations, we have generated essential gene deletion mutants, many of which are
631 also essential across multiple species (http://www.essentialgene.org/). These essential gene
632 mutants provide an invaluable resource for dissecting the functions of essential genes. Using

633 these twenty-four essential gene mutants and WT as controls, we identified over 1000
634 spontaneous suppressor mutations in passage experiments (Fig. 2). Leveraging these essential
635 gene mutants and distinct mutated segments, we constructed a functional network (Fig. 3a).
636 Within this network, we made several noteworthy observations. 1) Mutated segments that
637 appeared in the evolved WT population can also appear in the evolved populations of mutants
638 with deletions of essential genes, such as mutations in the PTS mannose/fructose/sorbose
639 transporter family subunit. 2) Suppressor mutations in certain genes, such as *rpoB* and *rpsL,* that
640 are found in the evolved populations of one deletion mutant can also be present in the evolved
641 populations of other mutants (Supplemental Table 4). 3) Mutual essential gene suppressor
642 mutations were discovered, where mutations in the first essential gene were found within a
643 mutant population deleted for the second essential gene, and vice versa.
644
645 As expected, our findings support the notion that mutants with deletions of essential genes face
646 stronger selective pressures when compared to that of the WT. These mutants are more likely to
647 undergo the following significant evolutionary changes. 1) Gene duplications of greater than 10
648 kb: Our data revealed large-scale gene duplications exclusively were present in mutants deleted
649 of essential genes (Fig. 2b-h). 2) Substitutions, insertions, and deletions of less than 10 kb:
650 Small-scale mutations, especially those of >50% of sequence reads, were more common in
651 mutants deleted for essential genes (Fig. 2i). 3) Mutations in essential genes: Mutations in other
652 essential genes were observed more exclusively in mutants deleted for an essential gene (Fig.
653 2k). 4) Mutations in multi-drug resistance genes: mutations of multi-drug resistance-associated
654 genes, such as *rpoB* and *rpsL,* are present in several evolved populations deleted for essential
655 genes, suggesting a shared selective pressure resulting from drug treatment and deletion of
656 essential genes (Supplemental Table 4). The suppressor mutations identified in our evolved
657 populations deleted of essential genes may reflect the differential gene essentiality over
658 evolutionary time in the pan-genome [11] and reproducibly changing gene essentiality across
659 independently evolving populations. [18]
660
661 Unexpectedly, as discussed above, for every essential gene mutated, we identified at least one
662 population containing a suppressor mutation in another essential gene (Fig. 2l). Notably, the
663 essential genes were inactivated by the suppressor mutation in some of the evolved populations,
664 such as the >200bp insertion mutation in *ftsZ* in the evolved population of *Δf1fo #107*, the >200
665 bp deletion mutation of *uncH* in *ΔuncC#1*, and the 1 bp deletion mutation of *ftsE* in *ΔftsX#13*
666 (Supplemental Table 4). In contrast, for other essential gene mutation suppressors, the mutations
667 were not within the open reading frame (ORF) but were found within 400 base pairs upstream of
668 the start codons, likely affecting expression rather than inactivating function. For instance, in the
669 evolved *ΔdpcK* populations, the suppressors with the highest mutation frequency were located
670 upstream of the holo-ACP synthase gene, *acpS* (Supplementary Fig.5). Similarly, in the evolved
671 *ΔobgE* populations, the majority of mutation suppressors were found upstream of *rpoB*
672 (Supplementary Fig.5).
673
674 Essential genes represent ideal drug targets for controlling infectious diseases and cancers. In
675 traditional medical treatment, the focus has primarily been on targeting a single essential gene
676 product. However, it's crucial to consider the evolution of gene essentiality during drug treatment
677 and the development of drug resistance over short-term evolution. We have observed that in
678 multiple populations deleted of essential genes, mutations in multiple segments appeared within

679 six passages, including those belonging to multi-drug resistance-associated genes (Fig. 2m).
680 Considering that some of the suppressor mutations were gene duplications that presumably
681 confer fitness benefits by increasing gene copy numbers, a promising approach is to target not
682 only the essential gene itself but also the backup gene. This strategy can help prevent or reduce
683 the development of drug resistance.
684
685 To understand the relationships between the structure and function of a protein, it is of great
686 interest to know which amino acids or domains of the proteins are sensitive to mutations. In this
687 study, we have observed numerous mutations of *trkA1* and *trkH1* in *Δf1fo* or *f1fo* single subunit
688 deletion mutants, *vicK* in *ΔftsX*, *fruR* and *glcK* in *ΔpfkA*, as well as *fusA*, *rpsL* and *rplF* in
689 kanamycin-resistant mutants lacking the *kan* gene (Supplemental Table 1-2). These mutations
690 represent fitness-related protein sequence changes that improve the growth of resultant mutants
691 in a particular selective condition.
692
693 In this work, we have demonstrated the efficacy of the methodology developed for generating
694 deletion mutants of numerous essential genes in *S. sanguinis* SK36. Furthermore, we have
695 highlighted the potency of experimental evolution [29,30] in unraveling the mechanisms of gene
696 essentiality, with a particular focus on *f1fo* in *S. sanguinis* and *S. mutans*. It would be interesting
697 to test the conservation or divergence of mechanisms governing gene essentiality of other genes,
698 as well as across different *Streptococcus* species and other genera. While extracting valuable
699 information by identifying spontaneous suppressor mutations in populations lacking essential
700 genes is possible, conducting experimental evolution requires caution. First and foremost, the
701 choice of an appropriate organism is crucial. Ideally, the selected organism should have a single
702 chromosome, a small genome size, and a rapid cell division rate. Streptococci represent an ideal
703 candidate in this regard. They possess a single circular genome with a relatively modest size,
704 typically ranging from 2.0 to 3.0 megabases. [77] This choice contrasts with a previous study that
705 employed budding yeast with multiple chromosomes [4] where most mutations in populations
706 lacking essential genes were related to changes in ploidy, which could hinder the identification
707 of causal suppressors. On the other hand, the identification of mechanisms of genetic suppression
708 requires caution. For the suppressor mutations of low frequency or these substitution mutations
709 where we were unable to determine whether the evolved suppressor mutations increase or
710 decrease the activity of the gene product, further evidence is needed to understand the
711 mechanisms underlying the evolution of gene essentiality.
712
713 In general, essential genes tend to be more conserved and evolutionarily ancient compared to
714 non-essential genes. [54] It is intriguing to consider when genes emerge within a biological system
715 over time. The suppressor mutations in essential gene mutants, particularly the loss-of-function
716 mutations, can provide valuable insights into dependency relationships. For instance, the absence
717 of *f1fo* in a system may hinder the emergence of the *trkA1-H1* system. In cases where essential
718 genes function as a complex, such as *f1fo* or *ftsEX*, our findings indicate that deletion of one
719 component may result in additional deleterious effects caused by the remaining subunit(s)
720 (Supplemental Table 4). This suggests that all subunits of the complex need to be integrated into
721 the system, at least for these cases. Moreover, understanding the timelines of gene emergence in
722 a system is also crucial for guiding decisions in synthetic biology, determining which genes, as
723 well as the order of genes, to be introduced into a system.
724

725 **Materials and Methods**
726
727 *Strains Used and Growth Conditions:*
728 In this study, we primarily utilized *Streptococcus sanguinis* strain SK36.[32] *S. sanguinis* SK405
729 and SK1058 strains were described previously.[38] *S. mutans* UA159 was obtained from Ann
730 Progulske-Fox (University of Florida). All bacterial cultures were routinely maintained in a BHI
731 medium at 37°C under anaerobic conditions, using a Coy anaerobic chamber, or stored at -80 °C
732 for long-term storage.
733
734 *Transformation and Mutant Isolation:*
735 To prepare competent cells, *S. sanguinis* was cultured in 1 mL of Todd-Hewitt + HS medium [10]
736 and incubated overnight in anaerobic conditions at 37°C. The following day, a 5 µL aliquot of
737 the overnight culture was added to 1 mL of fresh TS+HS medium and incubated for an additional
738 3 hours.
739
740 For creating knockout constructs, we employed 1 kb of homologous 3' and 5' end sequences
741 flanking the coding sequence (CDS) and resistance genes, *kan* or *Erm*^{r}, in overlapping extension
742 PCR (for primers used, see Supplemental Table 21).[32] For transformation, we mixed 50 ng to
743 500 ng of PCR product DNA with 200 ng of CSP and 300 µL of competent cells. The reactions
744 continued for 24 hours under anaerobic conditions at 37°C. Subsequently, transformation
745 reaction mixtures were plated on BHI-agar containing appropriate antibiotics (Kanamycin: 500
746 µg/mL or Erythromycin: 10 µg/mL) for selection. Once the plates had dried, the cells were
747 overlaid with a thin layer of agar by adding 1 mL of cooled BHI-agar with antibiotics. The plates
748 were incubated at 37°C under anaerobic conditions to select transformants for 4 to 5 days.
749
750 For genotyping, genomic DNA (gDNA) was isolated from 2 mL of saturated cultures. In brief,
751 cells were precipitated by centrifugation at 10,000 rpm for 10 minutes at room temperature. They
752 were then resuspended in 200 µL of resuspension buffer (20 mM EDTA, 200 mM Tris-HCl, and
753 2% Triton-X 100) and lysed with 200 µL of AL lysis buffer (Qiagen, 19075). DNA was
754 precipitated by adding 1 mL of 100% ethanol supplemented with 100 mM of sodium acetate.
755 Following washing and drying, the DNA was dissolved in 100 µL of water and used for PCR
756 and/or whole-genome sequencing.
757
758 To generate deletion mutants *Δf1fo* in *ΔtrkA1-H1* and *ΔtrkA2-H2*, the *ΔtrkA1-H1* and *ΔtrkA2-H2*
759 mutants were first generated using *Erm*^{r} (Supplementary Fig.10). After confirmation of deletion
760 of *ΔtrkA1-H1* and *ΔtrkA2-H2, Δf1fo* of *kan* resistance construct was subsequentially transformed
761 into *ΔtrkA1-H1* or *ΔtrkA2-H2.* To generate deletion mutants of both *trkA1-H1* and *trkA2-H2*,
762 *trkA1, trkH1*, or *ΔtrkA1-H1* of erythromycin resistance constructs were transformed into a
763 *ΔtrkH2* mutant of kan resistance background (Xu, et al., 2011). To isolate *Δf1fo* and *ΔtrkA1-H1*
764 mutants in the SK405 and SK1058 strains, we employed the same PCR construct used for
765 deleting *f1fo* and *trkA1-H1* in SK36, as there is >90% identity at the flanking regions between
766 SK36, SK1058, and SK405.
767
768 *Strain Passage:*
769 Antibiotic-resistant colonies from selection plates were transferred to 1 mL of BHI containing
770 antibiotics and grown for 2 to 8 days under anaerobic conditions at 37°C. The duration depended

771 on when the OD_{600} reached 0.1-0.5, which was referred to as P0. A 300 µL aliquot of the cell
772 culture was then transferred to 3 mL of BHI containing antibiotics, and growth continued until
773 saturation, resulting in P1. P1 was mixed by pipetting five times with a P-1000 pipette, and 50
774 µL of the mixed P1 was transferred to 1 mL of BHI containing antibiotics. Growth proceeded
775 until the cell culture reached an OD_{600} of 0.1 to 0.5, producing P2. The latter process was
776 repeated sequentially from P3 to P6, where the volume of P2 to P5 was 1 mL and the final
777 passage, P6 was 3 mL. Cell cultures of P1 and P6 were stored at -80°C in glycerol at the final
778 concentration of 20%. DNA extractions and genome sequencing were conducted in P6 and/or P1
779 when indicated.
780
781 For passages involving WT, glycerol stocks from -80°C were transferred to 1 mL of BHI and
782 grown for 24 hours, resulting in T0 (see Supplementary Fig.4a). A 50 µL aliquot of T0 cell
783 culture was aliquoted into six 1.5 mL tubes, each containing 1 mL of BHI, and grown for 24
784 hours, resulting in T1. A 50 µL aliquot of T1 cell culture was inoculated into 1 mL of BHI and
785 grown for 24 hours, leading to T2. This process was repeated for T3 to T9.
786
787 *Whole-Genome Sequencing and Variant Calling:*
788 Whole-genome sequencing was carried out by the Genome Core at Virginia Commonwealth
789 University or by SeqCenter (https://www.seqcenter.com/) using the shotgun method with 2x150
790 paired-end sequencing. Whole-genome sequences with an average coverage of ≥200 were used
791 for subsequent analysis.
792
793 Fastq files were aligned to the SK36 reference genome [16] using Geneious Prime software
794 (https://www.geneious.com/) after trimming via the BBDuk method. Variations in the genome
795 were exported from Geneious Prime. To identify the mutated segment, the frequencies
796 (percentages) of all mutations belonging to a certain segment were assessed and the greatest
797 value of percentages were assigned to that segment. For the deletions, the read coverages were
798 calculated by averaging the base coverages that were 100 bp from the flanking sequence. For
799 network analysis, the software Cytoscape was used.[78]
800
801 **Data and materials availability**
802 All data needed to evaluate the conclusions in the paper are present in the paper and/or the
803 Supplementary files. The genome sequence data will be deposited to BioProject
804 (PRJNA1146876). All the transgenic materials, including the essential gene deletion mutants are
805 available from the authors upon request.
806
807
808 **Contributions**
809
810 L.B. and P.X. conceived the project. L.B., T.K. and P.X. designed the experiments. L.B.
811 constructed all the essential gene mutants and performed all experimental evolution studies. L.B.,
812 T.K., and P.X. analyzed the data with the help of Z.Z., A.I., B.Z., V.A. and M.W. The
813 manuscript was written and revised by L.B., T.K., and P.X.
814
815
816 **Acknowledgments**

The authors would like to thank Dr. Mark Running at the Department of Biology, University of Louisville, Dr. Tomomichi Fujita at the Department of Biological Sciences, Hokkaido University, Dr. Tim van Opijnen at Broad Institute, MIT and Harvard, and Dr. Yan Bao at the School of Agriculture and Biology, Shanghai Jiao Tong University, for discussions regarding experimental design and critical reading of the manuscript. We also thank Dr. Junling Ren at the Philips Institute for Oral Health Research, Virginia Commonwealth University for help with network analysis and Ms. Ayana Wyche at Virginia Commonwealth University for assistance with the culturing of bacteria. We are grateful to Vladimir Lee and Kalyan Maliempati for genomic sequencing services. This work was funded by grants from the National Institutes of Health R01DE030121 (P.X. and T.K.) and the CCTR Endowment Fund (P.X.).

Declaration of generative AI in scientific writing

During the preparation of this work the authors used ChatGPT-3 in order to improve readability and language. After using it, the authors reviewed and edited the content as needed and took full responsibility for the content of the publication.

Declaration of interests

A patent application has been submitted by P.X. and L.B. and the Virginia Commonwealth University based on these results.

References

1. Xu, P., Ge, X., Chen, L., Wang, X., Dou, Y., Xu, J.Z., Patel, J.R., Stone, V., Trinh, M., Evans, K., et al. (2011). Genome-wide essential gene identification in *Streptococcus sanguinis*. Scientific reports *1*, 125. 10.1038/srep00125.
2. Rancati, G., Moffat, J., Typas, A., and Pavelka, N. (2018). Emerging and evolving concepts in gene essentiality. Nat Rev Genet *19*, 34-49. 10.1038/nrg.2017.74.
3. Zhang, Z., and Ren, Q. (2015). Why are essential genes essential? - The essentiality of *Saccharomyces genes*. Microb Cell *2*, 280-287. 10.15698/mic2015.08.218.
4. D'Elia, M.A., Pereira, M.P., and Brown, E.D. (2009). Are essential genes really essential? Trends Microbiol *17*, 433-438. 10.1016/j.tim.2009.08.005.
5. Brown, E.D., and Wright, G.D. (2016). Antibacterial drug discovery in the resistance era. Nature *529*, 336-343. 10.1038/nature17042.
6. Hogan, A.M., and Cardona, S.T. (2022). Gradients in gene essentiality reshape antibacterial research. FEMS Microbiol Rev *46*. 10.1093/femsre/fuac005.
7. Costanzo, M., VanderSluis, B., Koch, E.N., Baryshnikova, A., Pons, C., Tan, G., Wang, W., Usaj, M., Hanchard, J., Lee, S.D., et al. (2016). A global genetic interaction network maps a wiring diagram of cellular function. Science *353*. 10.1126/science.aaf1420.
8. Jana, B., Liu, X., Dénéréaz, J., Park, H., Leshchiner, D., Liu, B., Gallay, C., Veening, J.W., and van Opijnen, T. (2023). CRISPRi-TnSeq: A genome-wide high-throughput tool for bacterial essential-nonessential genetic interaction mapping. bioRxiv. 10.1101/2023.05.31.543074.

862 9. Nijman, S.M. (2011). Synthetic lethality: general principles, utility and detection using
863 genetic screens in human cells. FEBS Lett *585*, 1-6. 10.1016/j.febslet.2010.11.024.
864 10. Leaver, M., Domínguez-Cuevas, P., Coxhead, J.M., Daniel, R.A., and Errington, J.
865 (2009). Life without a wall or division machine in *Bacillus subtilis*. Nature *457*, 849-853.
866 10.1038/nature07742.
867 11. Mutschler, H., Gebhardt, M., Shoeman, R.L., and Meinhart, A. (2011). A novel
868 mechanism of programmed cell death in bacteria by toxin-antitoxin systems corrupts
869 peptidoglycan synthesis. PLoS Biol *9*, e1001033. 10.1371/journal.pbio.1001033.
870 12. Li, J., Wang, H.T., Wang, W.T., Zhang, X.R., Suo, F., Ren, J.Y., Bi, Y., Xue, Y.X., Hu,
871 W., Dong, M.Q., and Du, L.L. (2019). Systematic analysis reveals the prevalence and
872 principles of bypassable gene essentiality. Nat Commun *10*, 1002. 10.1038/s41467-019-
873 08928-1.
874 13. Larrimore, K.E., and Rancati, G. (2019). The conditional nature of gene essentiality in
875 *Pseudomonas aeruginosa*. Curr Opin Genet Dev *58-59*, 55-61.
876 10.1016/j.gde.2019.07.015.
877 14. Liu, G., Yong, M.Y., Yurieva, M., Srinivasan, K.G., Liu, J., Lim, J.S., Poidinger, M.,
878 Wright, G.D., Zolezzi, F., Choi, H., et al. (2015). Gene Essentiality Is a Quantitative
879 Property Linked to Cellular Evolvability. Cell *163*, 1388-1399.
880 10.1016/j.cell.2015.10.069.
881 15. Rancati, G., Pavelka, N., Fleharty, B., Noll, A., Trimble, R., Walton, K., Perera, A.,
882 Staehling-Hampton, K., Seidel, C.W., and Li, R. (2008). Aneuploidy underlies rapid
883 adaptive evolution of yeast cells deprived of a conserved cytokinesis motor. Cell *135*,
884 879-893. 10.1016/j.cell.2008.09.039.
885 16. Bao, L., Inoue, N., Ishikawa, M., Gotoh, E., Teh, O.K., Higa, T., Morimoto, T., Ginanjar,
886 E.F., Harashima, H., Noda, N., et al. (2022). A PSTAIRE-type cyclin-dependent kinase
887 controls light responses in land plants. Sci Adv *8*, eabk2116. 10.1126/sciadv.abk2116.
888 17. Rosconi, F., Rudmann, E., Li, J., Surujon, D., Anthony, J., Frank, M., Jones, D.S., Rock,
889 C., Rosch, J.W., Johnston, C.D., and van Opijnen, T. (2022). A bacterial pan-genome
890 makes gene essentiality strain-dependent and evolvable. Nat Microbiol *7*, 1580-1592.
891 10.1038/s41564-022-01208-7.
892 18. Couce, A., Limdi, A., Magnan, M., Owen, S.V., Herren, C.M., Lenski, R.E., Tenaillon,
893 O., and Baym, M. (2024). Changing fitness effects of mutations through long-term
894 bacterial evolution. Science *383*, eadd1417. 10.1126/science.add1417.
895 19. Santamaría, D., Barrière, C., Cerqueira, A., Hunt, S., Tardy, C., Newton, K., Cáceres,
896 J.F., Dubus, P., Malumbres, M., and Barbacid, M. (2007). Cdk1 is sufficient to drive the
897 mammalian cell cycle. Nature *448*, 811-815. 10.1038/nature06046.
898 20. Nowack, M.K., Harashima, H., Dissmeyer, N., Zhao, X.A., Bouyer, D., Weimer, A.K.,
899 De Winter, F., Yang, F., and Schnittger, A. (2012). Genetic framework of cyclin-
900 dependent kinase function in *Arabidopsis*. Dev. Cell *22*, 1030-1040.
901 10.1016/j.devcel.2012.02.015.
902 21. Glass, J.I., Merryman, C., Wise, K.S., Hutchison, C.A., and Smith, H.O. (2017). Minimal
903 Cells-Real and Imagined. Cold Spring Harb Perspect Biol *9*.
904 10.1101/cshperspect.a023861.
905 22. Juhas, M., Eberl, L., and Church, G.M. (2012). Essential genes as antimicrobial targets
906 and cornerstones of synthetic biology. Trends Biotechnol *30*, 601-607.
907 10.1016/j.tibtech.2012.08.002.

908 23. Hutchison, C.A., Chuang, R.Y., Noskov, V.N., Assad-Garcia, N., Deerinck, T.J.,
909 Ellisman, M.H., Gill, J., Kannan, K., Karas, B.J., Ma, L., et al. (2016). Design and
910 synthesis of a minimal bacterial genome. Science *351*, aad6253.
911 10.1126/science.aad6253.
912 24. Ratcliff, W.C., Denison, R.F., Borrello, M., and Travisano, M. (2012). Experimental
913 evolution of multicellularity. Proc Natl Acad Sci U S A *109*, 1595-1600.
914 10.1073/pnas.1115323109.
915 25. Blount, Z.D., Borland, C.Z., and Lenski, R.E. (2008). Historical contingency and the
916 evolution of a key innovation in an experimental population of Escherichia coli. Proc
917 Natl Acad Sci U S A *105*, 7899-7906. 10.1073/pnas.0803151105.
918 26. Moger-Reischer, R.Z., Glass, J.I., Wise, K.S., Sun, L., Bittencourt, D.M.C., Lehmkuhl,
919 B.K., Schoolmaster, D.R., Lynch, M., and Lennon, J.T. (2023). Evolution of a minimal
920 cell. Nature *620*, 122-127. 10.1038/s41586-023-06288-x.
921 27. Kawecki, T.J., Lenski, R.E., Ebert, D., Hollis, B., Olivieri, I., and Whitlock, M.C. (2012).
922 Experimental evolution. Trends Ecol Evol *27*, 547-560. 10.1016/j.tree.2012.06.001.
923 28. Barrick, J.E., and Lenski, R.E. (2013). Genome dynamics during experimental evolution.
924 Nat Rev Genet *14*, 827-839. 10.1038/nrg3564.
925 29. McDonald, M.J. (2019). Microbial Experimental Evolution - a proving ground for
926 evolutionary theory and a tool for discovery. EMBO Rep *20*, e46992.
927 10.15252/embr.201846992.
928 30. Van den Bergh, B., Swings, T., Fauvart, M., and Michiels, J. (2018). Experimental
929 Design, Population Dynamics, and Diversity in Microbial Experimental Evolution.
930 Microbiol Mol Biol Rev *82*. 10.1128/MMBR.00008-18.
931 31. Taylor, T.B., Mulley, G., Dills, A.H., Alsohim, A.S., McGuffin, L.J., Studholme, D.J.,
932 Silby, M.W., Brockhurst, M.A., Johnson, L.J., and Jackson, R.W. (2015). Evolutionary
933 resurrection of flagellar motility via rewiring of the nitrogen regulation system. Science
934 *347*, 1014-1017. 10.1126/science.1259145.
935 32. Xu, P., Alves, J.M., Kitten, T., Brown, A., Chen, Z., Ozaki, L.S., Manque, P., Ge, X.,
936 Serrano, M.G., Puiu, D., et al. (2007). Genome of the opportunistic pathogen
937 Streptococcus sanguinis. J Bacteriol *189*, 3166-3175. 10.1128/JB.01808-06.
938 33. Lázár, V., Pal Singh, G., Spohn, R., Nagy, I., Horváth, B., Hrtyan, M., Busa-Fekete, R.,
939 Bogos, B., Méhi, O., Csörgő, B., et al. (2013). Bacterial evolution of antibiotic
940 hypersensitivity. Mol Syst Biol *9*, 700. 10.1038/msb.2013.57.
941 34. Rhodes, D.V., Crump, K.E., Makhlynets, O., Snyder, M., Ge, X., Xu, P., Stubbe, J., and
942 Kitten, T. (2014). Genetic characterization and role in virulence of the ribonucleotide
943 reductases of Streptococcus sanguinis. J Biol Chem *289*, 6273-6287.
944 10.1074/jbc.M113.533620.
945 35. Luo, H., Lin, Y., Gao, F., Zhang, C.T., and Zhang, R. (2014). DEG 10, an update of the
946 database of essential genes that includes both protein-coding genes and noncoding
947 genomic elements. Nucleic Acids Res *42*, D574-580. 10.1093/nar/gkt1131.
948 36. Nelson, N., Perzov, N., Cohen, A., Hagai, K., Padler, V., and Nelson, H. (2000). The
949 cellular biology of proton-motive force generation by V-ATPases. J Exp Biol *203*, 89-95.
950 10.1242/jeb.203.1.89.
951 37. Röttig, A., and Steinbüchel, A. (2013). Acyltransferases in bacteria. Microbiol Mol Biol
952 Rev *77*, 277-321. 10.1128/MMBR.00010-13.

953 38. Baker, S.P., Nulton, T.J., and Kitten, T. (2019). Genomic, Phenotypic, and Virulence
954 Analysis of Streptococcus sanguinis Oral and Infective-Endocarditis Isolates. Infect
955 Immun *87*. 10.1128/IAI.00703-18.
956 39. Ghosh, A., N, S., and Saha, S. (2020). Survey of drug resistance associated gene
957 mutations in Mycobacterium tuberculosis, ESKAPE and other bacterial species.
958 Scientific reports *10*, 8957. 10.1038/s41598-020-65766-8.
959 40. Zeng, L., Walker, A.R., Lee, K., Taylor, Z.A., and Burne, R.A. (2021). Spontaneous
960 Mutants of Streptococcus sanguinis with Defects in the Glucose-Phosphotransferase
961 System Show Enhanced Post-Exponential-Phase Fitness. J Bacteriol *203*, e0037521.
962 10.1128/JB.00375-21.
963 41. Chevin, L.M., Martin, G., and Lenormand, T. (2010). Fisher's model and the genomics of
964 adaptation: restricted pleiotropy, heterogenous mutation, and parallel evolution.
965 Evolution *64*, 3213-3231. 10.1111/j.1558-5646.2010.01058.x.
966 42. Wichman, H.A., Badgett, M.R., Scott, L.A., Boulianne, C.M., and Bull, J.J. (1999).
967 Different trajectories of parallel evolution during viral adaptation. Science *285*, 422-424.
968 10.1126/science.285.5426.422.
969 43. Stern, D.L. (2013). The genetic causes of convergent evolution. Nat Rev Genet *14*, 751-
970 764. 10.1038/nrg3483.
971 44. Sheng, J., and Marquis, R.E. (2006). Enhanced acid resistance of oral streptococci at
972 lethal pH values associated with acid-tolerant catabolism and with ATP synthase activity.
973 FEMS Microbiol Lett *262*, 93-98. 10.1111/j.1574-6968.2006.00374.x.
974 45. Corratgé-Faillie, C., Jabnoune, M., Zimmermann, S., Véry, A.A., Fizames, C., and
975 Sentenac, H. (2010). Potassium and sodium transport in non-animal cells: the
976 Trk/Ktr/HKT transporter family. Cell Mol Life Sci *67*, 2511-2532. 10.1007/s00018-010-
977 0317-7.
978 46. Du, S., Pichoff, S., and Lutkenhaus, J. (2016). FtsEX acts on FtsA to regulate divisome
979 assembly and activity. Proc Natl Acad Sci U S A *113*, E5052-5061.
980 10.1073/pnas.1606656113.
981 47. Moraes, J.J., Stipp, R.N., Harth-Chu, E.N., Camargo, T.M., Höfling, J.F., and Mattos-
982 Graner, R.O. (2014). Two-component system VicRK regulates functions associated with
983 establishment of Streptococcus sanguinis in biofilms. Infect Immun *82*, 4941-4951.
984 10.1128/IAI.01850-14.
985 48. Sham, L.T., Barendt, S.M., Kopecky, K.E., and Winkler, M.E. (2011). Essential PcsB
986 putative peptidoglycan hydrolase interacts with the essential FtsXSpn cell division
987 protein in *Streptococcus pneumoniae* D39. Proc Natl Acad Sci U S A *108*, E1061-1069.
988 10.1073/pnas.1108323108.
989 49. Gupta, A., Singh, P.K., Sharma, P., Kaur, P., Sharma, S., and Singh, T.P. (2020).
990 Structural and biochemical studies of phosphopantetheine adenylyltransferase from
991 *Acinetobacter baumannii* with dephospho-coenzyme A and coenzyme A. Int J Biol
992 Macromol *142*, 181-190. 10.1016/j.ijbiomac.2019.09.090.
993 50. Heath, R.J., and Rock, C.O. (1996). Inhibition of beta-ketoacyl-acyl carrier protein
994 synthase III (FabH) by acyl-acyl carrier protein in Escherichia coli. The Journal of
995 biological chemistry *271*, 10996-11000. 10.1074/jbc.271.18.10996.
996 51. Phong, W.Y., Lin, W., Rao, S.P., Dick, T., Alonso, S., and Pethe, K. (2013).
997 Characterization of phosphofructokinase activity in *Mycobacterium tuberculosis* reveals
998 that a functional glycolytic carbon flow is necessary to limit the accumulation of toxic

999 metabolic intermediates under hypoxia. PLoS One *8*, e56037.
1000 10.1371/journal.pone.0056037.
1001 52. Skarlatos, P., and Dahl, M.K. (1998). The glucose kinase of Bacillus subtilis. J Bacteriol
1002 *180*, 3222-3226. 10.1128/JB.180.12.3222-3226.1998.
1003 53. Boulanger, E.F., Sabag-Daigle, A., Thirugnanasambantham, P., Gopalan, V., and Ahmer,
1004 B.M.M. (2021). Sugar-Phosphate Toxicities. Microbiol Mol Biol Rev *85*, e0012321.
1005 10.1128/MMBR.00123-21.
1006 54. Zeng, L., and Burne, R.A. (2021). Molecular mechanisms controlling fructose-specific
1007 memory and catabolite repression in lactose metabolism by Streptococcus mutans. Mol
1008 Microbiol *115*, 70-83. 10.1111/mmi.14597.
1009 55. Morrissey, A.T., and Fraenkel, D.G. (1972). Suppressor of phosphofructokinase
1010 mutations of Escherichia coli. J Bacteriol *112*, 183-187. 10.1128/jb.112.1.183-187.1972.
1011 56. Babul, J. (1978). Phosphofructokinases from Escherichia coli. Purification and
1012 characterization of the nonallosteric isozyme. The Journal of biological chemistry *253*,
1013 4350-4355.
1014 57. Deckers, B., Vercauteren, S., De Kock, V., Martin, C., Lazar, T., Herpels, P., Dewachter,
1015 L., Verstraeten, N., Peeters, E., Ballet, S., et al. (2023). YbiB: a novel interactor of the
1016 GTPase ObgE. Nucleic Acids Res *51*, 3420-3435. 10.1093/nar/gkad127.
1017 58. Vidwans, S.J., Ireton, K., and Grossman, A.D. (1995). Possible role for the essential
1018 GTP-binding protein Obg in regulating the initiation of sporulation in Bacillus subtilis. J
1019 Bacteriol *177*, 3308-3311. 10.1128/jb.177.11.3308-3311.1995.
1020 59. Okamoto, S., Itoh, M., and Ochi, K. (1997). Molecular cloning and characterization of
1021 the obg gene of Streptomyces griseus in relation to the onset of morphological
1022 differentiation. J Bacteriol *179*, 170-179. 10.1128/jb.179.1.170-179.1997.
1023 60. Okamoto, S., and Ochi, K. (1998). An essential GTP-binding protein functions as a
1024 regulator for differentiation in Streptomyces coelicolor. Mol Microbiol *30*, 107-119.
1025 10.1046/j.1365-2958.1998.01042.x.
1026 61. Verstraeten, N., Knapen, W.J., Kint, C.I., Liebens, V., Van den Bergh, B., Dewachter, L.,
1027 Michiels, J.E., Fu, Q., David, C.C., Fierro, A.C., et al. (2015). Obg and Membrane
1028 Depolarization Are Part of a Microbial Bet-Hedging Strategy that Leads to Antibiotic
1029 Tolerance. Molecular cell *59*, 9-21. 10.1016/j.molcel.2015.05.011.
1030 62. Feng, B., Mandava, C.S., Guo, Q., Wang, J., Cao, W., Li, N., Zhang, Y., Wang, Z., Wu,
1031 J., Sanyal, S., et al. (2014). Structural and functional insights into the mode of action of a
1032 universally conserved Obg GTPase. PLoS Biol *12*, e1001866.
1033 10.1371/journal.pbio.1001866.
1034 63. Murti, K.G., Webster, R.G., and Jones, I.M. (1988). Localization of RNA polymerases on
1035 influenza viral ribonucleoproteins by immunogold labeling. Virology *164*, 562-566.
1036 10.1016/0042-6822(88)90574-0.
1037 64. Zielke, R., Sikora, A., Dutkiewicz, R., Wegrzyn, G., and Czyż, A. (2003). Involvement of
1038 the cgtA gene function in stimulation of DNA repair in Escherichia coli and Vibrio
1039 harveyi. Microbiology (Reading) *149*, 1763-1770. 10.1099/mic.0.26292-0.
1040 65. Czyz, A., Zielke, R., Konopa, G., and Wegrzyn, G. (2001). A Vibrio harveyi insertional
1041 mutant in the cgtA (obg, yhbZ) gene, whose homologues are present in diverse organisms
1042 ranging from bacteria to humans and are essential genes in many bacterial species.
1043 Microbiology (Reading) *147*, 183-191. 10.1099/00221287-147-1-183.

1044 66. Courcelle, J., Khodursky, A., Peter, B., Brown, P.O., and Hanawalt, P.C. (2001).
1045 Comparative gene expression profiles following UV exposure in wild-type and SOS-
1046 deficient Escherichia coli. Genetics *158*, 41-64. 10.1093/genetics/158.1.41.
1047 67. Foti, J.J., Persky, N.S., Ferullo, D.J., and Lovett, S.T. (2007). Chromosome segregation
1048 control by Escherichia coli ObgE GTPase. Mol Microbiol *65*, 569-581. 10.1111/j.1365-
1049 2958.2007.05811.x.
1050 68. Tan, J., Jakob, U., and Bardwell, J.C. (2002). Overexpression of two different GTPases
1051 rescues a null mutation in a heat-induced rRNA methyltransferase. J Bacteriol *184*, 2692-
1052 2698. 10.1128/JB.184.10.2692-2698.2002.
1053 69. Nirody, J.A., Budin, I., and Rangamani, P. (2020). ATP synthase: Evolution, energetics,
1054 and membrane interactions. J Gen Physiol *152*. 10.1085/jgp.201912475.
1055 70. Lund, P., Tramonti, A., and De Biase, D. (2014). Coping with low pH: molecular
1056 strategies in neutralophilic bacteria. FEMS Microbiol Rev *38*, 1091-1125. 10.1111/1574-
1057 6976.12076.
1058 71. Wang, Y., Wu, J., Lv, M., Shao, Z., Hungwe, M., Wang, J., Bai, X., Xie, J., and Geng,
1059 W. (2021). Metabolism Characteristics of Lactic Acid Bacteria and the Expanding
1060 Applications in Food Industry. Front Bioeng Biotechnol *9*, 612285.
1061 10.3389/fbioe.2021.612285.
1062 72. Ajdic, D., McShan, W.M., McLaughlin, R.E., Savic, G., Chang, J., Carson, M.B.,
1063 Primeaux, C., Tian, R., Kenton, S., Jia, H., et al. (2002). Genome sequence of
1064 Streptococcus mutans UA159, a cariogenic dental pathogen. Proc Natl Acad Sci U S A
1065 *99*, 14434-14439. 10.1073/pnas.172501299.
1066 73. Chen, P., Wang, D., Chen, H., Zhou, Z., and He, X. (2016). The nonessentiality of
1067 essential genes in yeast provides therapeutic insights into a human disease. Genome Res
1068 *26*, 1355-1362. 10.1101/gr.205955.116.
1069 74. Mnaimneh, S., Davierwala, A.P., Haynes, J., Moffat, J., Peng, W.T., Zhang, W., Yang,
1070 X., Pootoolal, J., Chua, G., Lopez, A., et al. (2004). Exploration of essential gene
1071 functions via titratable promoter alleles. Cell *118*, 31-44. 10.1016/j.cell.2004.06.013.
1072 75. Peters, J.M., Colavin, A., Shi, H., Czarny, T.L., Larson, M.H., Wong, S., Hawkins, J.S.,
1073 Lu, C.H.S., Koo, B.M., Marta, E., et al. (2016). A Comprehensive, CRISPR-based
1074 Functional Analysis of Essential Genes in Bacteria. Cell *165*, 1493-1506.
1075 10.1016/j.cell.2016.05.003.
1076 76. Shields, R.C., Walker, A.R., Maricic, N., Chakraborty, B., Underhill, S.A.M., and Burne,
1077 R.A. (2020). Repurposing the Streptococcus mutans CRISPR-Cas9 System to Understand
1078 Essential Gene Function. PLoS Pathog *16*, e1008344. 10.1371/journal.ppat.1008344.
1079 77. Yother, J., Trieu-Cuot, P., Klaenhammer, T.R., and De Vos, W.M. (2002). Genetics of
1080 streptococci, lactococci, and enterococci: review of the sixth international conference. J
1081 Bacteriol *184*, 6085-6092. 10.1128/JB.184.22.6085-6092.2002.
1082 78. Otasek, D., Morris, J.H., Bouças, J., Pico, A.R., and Demchak, B. (2019). Cytoscape
1083 Automation: empowering workflow-based network analysis. Genome Biol *20*, 185.
1084 10.1186/s13059-019-1758-4.
1085
1086 **Figures and legends**
1087
1088 **Figure 1. Evolution of mutants deleted for essential genes in passage experiments.**
1089

1090
1091 (a) Two types of colonies, small and large, as demonstrated for *f1fo* deletion, appear on selection
1092 plates after 5 days of growth. Only the small colonies represent true deletions, denoted as Δ*f1fo*
1093 (red circle). The large colonies are "double-band mutants," containing both the replacement of
1094 the original *f1fo* with a *kan* gene and a wild-type *f1fo* copy, or they are mutants that did not
1095 contain a *kan* gene, but contained point mutations in other genes, denoted as Δ*f1fo-DB* (black
1096 circle, 'DB' for double-band).
1097
1098 (b) Schematic representation of the passage experiments (see Materials and Methods). The
1099 numbers on the arrows indicate the dilution ratios for each passage. Images inserted below the
1100 passages show genome alignments to the reference at P1 or P6, with mismatches marked by a
1101 star (demonstrated using the *trkH1* mutation in the *Δf1fo#104* population shown in Figure 3d).
1102
1103 (c) Incubation time (days) required for P0 and P6 mutants to reach an OD_{600} of 0.1 to 0.5.
1104
1105
1106 **Figure 2. Identification of suppressors in mutants deleted for essential genes.**
1107
1108 (a) Number of independently evolved populations of different mutants.
1109
1110 (b-i) Evolved populations containing large-scale duplications. Red arrow, site of original
1111 essential gene deletion; Y axis indicates number of sequence reads mapped to the
1112 reference sequence at the coordinates shown on X axis.
1113
1114 (j) Boxplot of mutated segments (≥30% abundance) in the independently evolved populations of
1115 mutants deleted for essential genes or WT. Open circles indicate outliers.
1116
1117 (k) Stacked proportions of populations containing mutated segments comprising >50% (blue) or
1118 30%-50% (red) of sequence reads.
1119
1120 (l) Stacked proportions of mutated segments belonging to intergenic regions, non-essential
1121 ORFs, or essential ORFs.
1122
1123 (m) Stacked proportions of evolved populations with/without mutations in the multi-drug
1124 resistance genes (DRGs: *rpsL*, *gyrB*, *rpoB* and *rrs2*) shown.
1125
1126
1127 **Figure 3. Networks derived from the mutations in the evolved populations.**
1128
1129 **(a)** A network was built from the lists of suppressor mutants derived from each essential gene
1130 mutant and WT. Yellow-highlighted labels indicate the names of the essential genes mutated and
1131 the blue-highlighted label indicates the passaged WT. In total, there are twenty-five groups. Gene
1132 names without any marks, mutated segments belonging to essential genes; gene names with an
1133 asterisk (*) on the left, conditional essential genes; gene name with two asterisks on the left, non-
1134 essential genes; P_ followed by gene names and an asterisk, promoters; In_ followed by gene

1135 names and an asterisk and int_ followed by number, intergenic regions; _ followed by number,
1136 gene locus.
1137
1138 (b) Most commonly mutated segments in the evolved populations deleted of essential genes. Red
1139 cross on the rectangle boxes indicates evolved populations deleted of essential genes. Labels
1140 within the rectangle boxes indicate the segments with mutations. Numbers on top of the
1141 rectangle boxes indicate number of populations with mutations in the segments out of the total
1142 populations. Arrows indicate the flow of biochemical reactions.
1143
1144
1145 **Figure 4. Increasing *v1vo* copy number and inhibition of *trkA1-H1* independently**
1146 **contribute to the fitness improvement of evolved *Δf1fo* populations.**
1147
1148 (a) Gene duplication of *v1vo* region does not occur in P1 population (upper) and appeared in P6
1149 (lower) population of *Δf1fo#109.* Yellow arrows indicate passaging process. The black box
1150 indicates the *f1fo* region.
1151
1152 (b) Population of *Δf1fo#4* at P6 that does not contain gene duplication of *v1vo* region (upper).
1153 *v1vo* region duplication was observed in P15 (lower). (Two out of sixed evolved populations; see
1154 S7). Arrows indicate passaging process.
1155
1156 (c) *v1vo* region deleted in WT (upper). Duplication of *v1vo* region *Δf1fo#4, denoted as v1vo-DB/*
1157 *Δf1fo#4.* The black box indicates the *f1fo* region. The red box indicates *v1vo* region.
1158
1159 (d) Mutation frequency in *trkH1* increased with passage in P6 compared to P1 in population
1160 *Δf1f*#104.
1161
1162 (e) Growth of strains indicated. 0.1 OD_{600} of cells in a volume of 2 µl were spotted directly (first
1163 column) or diluted 20-fold (column 2), or 400-fold (column 3) and grown on BHI-agar for two
1164 days.
1165
1166 (f) Growth of the strains indicated. 0.1 OD_{600} of cells in a volume of 2 µl were spotted directly
1167 (first column) or diluted 10-fold (column 2), or 100-fold (column 3), or 1000-fold (column 4),
1168 and grown for four days.
1169
1170 (g) Quantitative growth measurements of WT, *ΔtrkA1-H1, ΔtrkA2-H2, Δf1fo* in *ΔtrkA1-H1* and
1171 *Δf1fo* in *ΔtrkA2-H2.* Culture is in BHI for 24 hr in anaerobic conditions. Data are shown as
1172 means ± SD from three replicate cultures. Different letters indicate statistically significant
1173 differences ($P \leq 0.05$), determined by one -way ANOVA with Tukey multiple comparisons test.
1174
1175 (h) Sensitivity of *Δf1fo#4* and WT to low pH (lactic acid: LA). The values are relative OD_{600} to
1176 that of WT grown in plain BHI. X-axis denotes the vol (µL) of 90% LA in 25 mL of BHI. Data
1177 are shown as means ± SD from three replicate cultures.
1178

1179 (i) Sensitivity of *Δf1fo#4* and WT to high pH (NaOH). The values are relative OD_{600} to that of
1180 WT grown in plain BHI. X-axis denotes the vol (μL) of 5 M NaOH in 25 mL of BHI. Data are
1181 shown as means ± SD from three replicate cultures.
1182
1183
1184
1185
1186 **Figure 5 Essentiality of *f1fo* in *S. mutans* UA159, *S. sanguinis* SK36, SK405 and SK1058.**
1187
1188 (a) Distribution of the genes indicated in *S. mutans* UA159, *S. sanguinis* SK36, SK405 and
1189 SK1058.
1190
1191 (b) Growth of *Δf1fo* transformants in *S. sanguinis* SK405 (upper) and SK1058 (lower) on same
1192 BHI agar medium for five days. Enlarged images of the transformants are shown. Red circles
1193 indicate small colonies, *Δf1fo*. Black circles indicate big colonies, *Δf1fo-DB*.
1194
1195 (c) Deletion of *f1fo* in SK405 or SK1058 shown by whole genome sequencing. Black box
1196 indicates the location of *f1fo* region.
1197
1198 (d) Quantitative measurements of growth in wild-type SK36, SK405 or SK1058, *ΔtrkA1-H1* or
1199 *Δf1fo* mutants in the backgrounds of SK36, SK405 or SK1058. Cells were grown in BHI for 24
1200 hours. Data are shown as means ± SD from three replicate cultures. Different letters indicate
1201 statistically significant differences ($P \leq 0.05$), determined by one -way ANOVA with Tukey
1202 multiple comparisons test.
1203
1204 (e) Growth of SK36, SK405 or SK1058, *ΔtrkA1-H1* mutant in the backgrounds of SK36, SK405
1205 or SK1058. 0.1 OD_{600} of cells in a volume of 2 μl were spotted directly (first column) or diluted
1206 10-fold (column 2), or 100-fold (column 3), or 1000-fold (column 4). Growth of Cells were
1207 grown on BHI-agar for two days.
1208
1209 (f) Growth of SK36, SK405 or SK1058, *Δf1fo* mutant in the backgrounds of SK36, SK405 or
1210 SK1058. Cells were diluted as in Fig. E and grown on BHI-agar for four days.
1211
1212 (g) Location of *trkA1-H1* suppressor mutations in SK405 and SK1058. Mutation of *trkA1-H1*
1213 appeared in all evolved *Δf1fo* populations, three in SK405 and two in SK1058. X-axis indicates
1214 the genome coordinates.
1215
1216
1217 **Supplemental Figures, Tables and legends**
1218
1219
1220 **Supplementary Fig.1. Genotyping and complementation of mutants deleted of *f1fo*.**
1221
1222 (a) Gene knockout strategy to delete entire region of eight *f1fo* subunits by homologous
1223 recombination. The yellow blocks indicate the eight F1Fo subunit genes in WT (upper). The blue
1224 block indicates the *kan* gene in Δ*f1fo* mutants (lower).

1225
1226 (b) Whole-genome sequencing to confirm the genotypes of the small colonies for Δ*f1fo* mutants.
1227 Black box indicates the location of deleted *f1fo* region. Enlarged image showed alignment of
1228 sequencing reads to the reference genome of *S. sanguinis* SK36. The blue graphic above the
1229 sequence coordinates (indicated by a red arrow) indicates the extent of coverage, the yellow bars
1230 indicate the mismatches (indicated by a star), and the bracket indicates the aligned sequence
1231 reads.
1232
1233 (c) Whole-genome sequencing of the big colonies, Δ*f1fo*-DB. Black box indicates the location of
1234 *f1fo* region. Red arrows indicate the two directly repeated *ugpC* genes, encoding glycerol-3-
1235 phosphate ABC transporter.
1236
1237
1238 **Supplementary Fig.2. Isolation of viable mutants deleted essential genes and genotyping by**
1239 **whole-genome sequencing.**
1240
1241 (a-b) Colonies of transformants (left) and whole-genome sequencing of colonies (right). Red
1242 circles indicate the colonies picked for whole-genome sequencing (left). For genome sequencing
1243 (right), the blue graphic above the sequence coordinates (indicated by a red arrow in the top
1244 panel of a.1) indicates the extent of coverage, the yellow bars indicate the mismatches, and the
1245 bracket indicates the aligned sequence reads. Bacterial colonies on selective agar plate for five
1246 days. (a.1-a.2) Gene deletion mutants with severe growth defects. (b) Gene deletion mutants with
1247 robust growth. Scale bar: 1 mm. The image of Δ*f1fo* transformation is a duplicate of Figure 1B to
1248 demonstrate the transformants in selection medium Δ*f1fo* alignment is a duplication of Fig.S1c.
1249
1250
1251 **Supplementary Fig.3. Growth of mutants deleted of essential genes, relative to that of WT.**
1252
1253 (a-b) Growth mutants deleted of 23 essential genes under anaerobic condition (a) and
1254 microaerobic condition (b). 0.1 OD_{600} of cells in a volume of 2 µl were spotted directly (first
1255 column) or diluted 20-fold (column 2), or 400-fold (column 3) and grown on BHI-agar for two
1256 days. Scale bar is 1 cm.
1257
1258 (c) Comparison of the growth of the twenty-four evolved mutants and that of WT. The values are
1259 relative OD_{600} after 24 hr of growth in BHI liquid medium.
1260
1261
1262 **Supplementary Fig.4. Large scale gene duplication present in the evolved populations of**
1263 **the mutants deleted essential genes but not in WT populations.**
1264
1265 (a) Whole-genome sequencing of parental WT and the six evolved WT populations after nine
1266 passages. The yellow arrow indicates the passage procedure.
1267
1268 (b-e) Evolved populations that contain gene duplication of greater than 10 kb in Δ*uncE#3* (b),
1269 Δ*f1fo#107* (c), Δ*fabH#4* (d) *and* Δ*fabH#6* (e). Red arrows (b-e) indicate the location of the gene

1270 intentionally deleted. The insert image (c) is an enlarged segments of *uncE* region, shown as a
1271 black box.
1272
1273
1274 **Supplementary Fig.S5. Appearance of mutations in essential genes in the evolved**
1275 **populations of strains intentionally deleted for different essential genes.**
1276
1277 (a-f) Aligned sequence reads from *ΔuncC#1* of P1 population (a-c) and P6 population (d-f). Red
1278 arrows indicate the deleted *uncC* in the genome (a and d) in the *ΔuncC#1* strain. Red box
1279 indicates mutation of *uncH* in *ΔuncC#1* (a and d). Enlarged mutated *uncH* region of aligned
1280 sequence reads in *ΔuncC#1* of P1 population (b-c) and P6 population (e-f). The yellow arrow
1281 indicates the passage procedure.
1282
1283 (g) Sequencing of the mutated *uncH* gene in *ΔuncC#1* in P6. Red letters indicate a fragment (82
1284 bp) that was present in mutated *uncH* gene (upper). Asterisk (*) indicates the stop codon that was
1285 highlighted. Vertical bars indicate the coordinates of the *uncH* ORF (lower). The coordinates
1286 between two red bars indicate replaced region.
1287
1288 (h-k) Aligned sequence reads from *Δf1fo#107* of P1 population (h-i) and P6 population (j-k). Red
1289 arrows indicate the deleted *f1fo* in the genome (h and j) in the *Δf1fo#107*. Red box indicates
1290 mutation of *ftsZ* in *Δf1fo#107* (h and j). Enlarged mutated *ftsZ* region of aligned sequence reads
1291 in *Δf1fo#107* of P1 population (h) and P6 population (i). The yellow arrow indicates the passage
1292 procedure. Supplementary Fig.5J is a duplicate of Supplementary Fig.4B to show a genome
1293 alignment of *Δf1fo#107* of P6.
1294
1295 (l) Sequencing of the mutated *ftsZ* in *Δf1fo#107* in P6. Red letters indicate a fragment (248 bp)
1296 that was present in mutated *Δf1fo#107* (upper). Asterisk (*) indicates the stop codon that was
1297 highlighted. Vertical bars indicated the coordinates of the *uncH* ORF (lower). The red bar
1298 indicates the coordinate where insertion occurred.
1299
1300
1301 **Supplementary Fig.6. Populations with and without mutations in three PTS**
1302 **mannose/fructose/sorbose transporter subunits.**
1303
1304 (a-b) Number (a) and percentage (b) of populations that have mutations in any of three PTS
1305 mannose/fructose/sorbose transporter subunits, namely J1C87_09355, J1C87_09360, and
1306 J1C87_09365.
1307
1308 **Supplementary Fig.7. The most frequent suppressors identified in mutants deleted of**
1309 **essential genes.**
1310 The percentage of mutated segments in evolved populations in *Δf1fo*, mutants deleted of single
1311 *unc* subunit genes, denoted as *Δf1fo.s*, the other single mutants indicated, and WT. The names
1312 with an asterisk (*) indicate the intergenic regions.
1313
1314

1315 **Supplementary Fig.8. Appearance of *v1vo* region gene duplication during passage. (Related**
1316 **to Figure 4a and 4b)**
1317
1318 (a-b) Alignment of sequence reads in populations of *Δf1fo#107, Δf1fo#109, uncE#2* and *uncH#7*
1319 at P1 (A) and P6 (B). The black box indicates the deleted *f1fo* region and the red arrows indicate
1320 the deleted *uncE* or *uncH.*
1321
1322 (c) Alignment of sequence reads of the P6 population in *Δf1fo#4* (upper) and five derived
1323 populations from P15 (lower). Rectangles represent the deleted *f1fo* region. Asterisks (*) indicate
1324 the two populations with *v1vo* region gene duplications.
1325
1326
1327 **Supplementary Fig.9. Gene duplication in *Δv1vo-DB/Δf1fo#4* populations (related to Figure**
1328 **4c).**
1329
1330 Alignment of sequence reads of five additional *Δv1vo-DB/Δf1fo#4* populations. The black box
1331 indicates the deleted *f1fo*. The red box indicates the gene duplication of *v1vo* region when one
1332 copy of *v1vo* was deleted.
1333
1334
1335 **Supplementary Fig.10. Alignment of sequence reads of *trk* mutants with and without *f1fo***
1336 **deletion**.
1337
1338 (a-k) Alignment of sequence reads of *ΔtrkA1* (a), *ΔtrkH1* (b), *ΔtrkA1-H1* (c), *ΔtrkA2* (d), *ΔtrkH2*
1339 (e), *ΔtrkA2-H2* (f), *ΔtrkA1/ΔtrkH2* (g), *ΔtrkH1/ΔtrkH2* (h), *ΔtrkA1-H1/ΔtrkH2* (i), *Δf1fo/ΔtrkA1-*
1340 *H1* (j), and *Δf1fo/ΔtrkA2-H2* (k). Red arrows indicated intended gene deletion. The block box
1341 indicates the deleted *f1fo region.* (related to Figure 4f).
1342
1343 **Supplementary Fig.11. Working model for F1Fo, V1Vo, TrkA1-H1 and TrkA2-H2.**
1344
1345 For streptococci, which do not contain a complete tricarboxylic acid cycle (TCA: shaded) or
1346 electron transport chain (ETC: shaded), energy production is mainly through lactic acid
1347 fermentation. The lactate from fermentation creates acidic conditions in the cytosol, which
1348 becomes toxic if H+ is not exported. F1Fo pumps out H+ from the cytosol using ATP, and V1Vo
1349 supplements or replaces the function of F1Fo when the F1Fo is inhibited/inactivated. Both
1350 TrkA1-H1 and TrkA2-H1 are potassium transporters, and functionally redundant. TrkA1-H1
1351 pumps in potassium together with H+, acidifying the cytosol when H+ is not exported. In
1352 contrast, TrkA2-H2 does not pump protons into the cytosol when pumping in potassium (likely
1353 instead pumping in Na+). Therefore, the function of TrkA1-H1 must be inhibited if F1Fo is not
1354 functional. Solid lines indicate presence of reactions. Dashed lines indicate absence of reactions.
1355
1356 **Supplementary Fig.12. *f1fo* cannot be deleted in *S. mutans* UA159.**
1357
1358 (a) Gene knockout strategy to delete entire region of eight *f1fo* subunits by homologous
1359 recombination. The purple blocks indicate the eight F1Fo subunit genes in WT (upper). The blue

1360 block indicates the *kan* gene in Δ*f1fo* mutants (lower). The two arrows indicate the primer set for
1361 the PCR amplicon of the region in (B).
1362
1363 (b) Genotyping the presence of wild-type *f1fo* colonies from selection medium. P: positive
1364 control using DNA template from wild-type. N: negative control using water as a template. The
1365 size of amplicons is about 1300 bp.
1366
1367
1368 **Supplementary Fig.13. Deletion *of trkA1-H1* in *S. sanguinis* SK1058 and S. sanguinis**
1369 **SK405 (related to Figure 5c).**
1370
1371 (a-b) Alignment of sequence reads of *ΔtrkA1-H1* populations in SK405 (a) and in SK1058 (b)
1372 backgrounds.
1373
1374
1375 **Supplementary Fig.14. Deletion *of f1fo* in *S. sanguinis* SK1058 and SK405 (related to**
1376 **Figure 5c).**
1377 Alignment of sequence reads of three *Δf1fo* populations in SK405 backgrounds (a) and two in
1378 SK1058 backgrounds (b) (related to Figure 5c). Rectangles represent the deleted *f1fo* region.

Fig.1

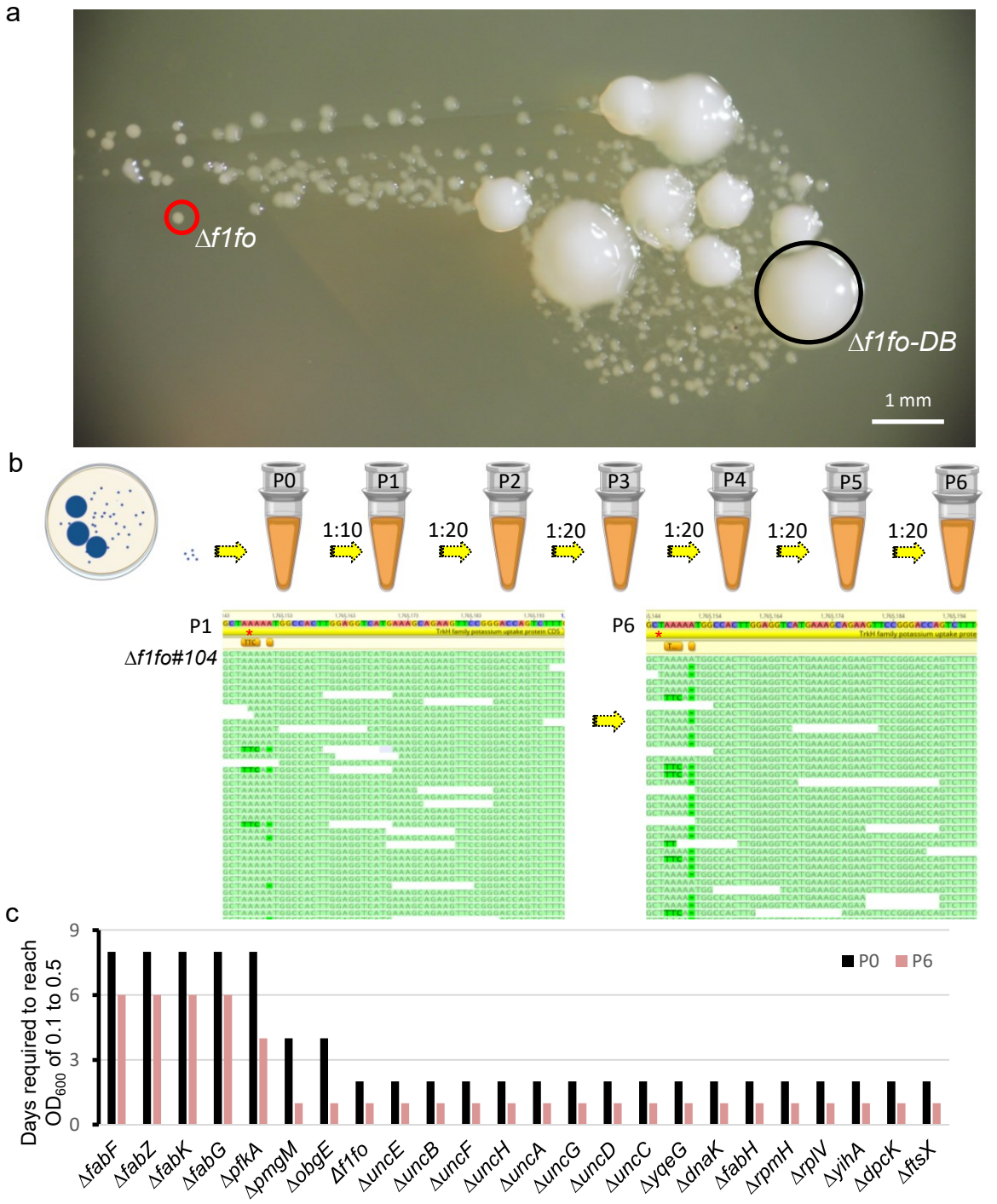
a
Δf1fo
Δf1fo-DB
1 mm
b
P0
P1
P2
P3
P4
P5
P6
1:10
1:20
1:20
1:20
1:20
1:20
P1
Δf1fo#104
P6
c
Days required to reach OD600 of 0.1 to 0.5
9
6
3
0
P0
P6
ΔfabF
ΔfabZ
ΔfabK
ΔfabG
ΔpfkA
ΔpmgM
ΔobgE
Δf1fo
ΔuncE
ΔuncB
ΔuncF
ΔuncH
ΔuncA
ΔuncG
ΔuncD
ΔuncC
ΔyqeG
ΔdnaK
ΔfabH
ΔrpmH
ΔrplV
ΔyihA
ΔdpcK
ΔftsX

Fig.2

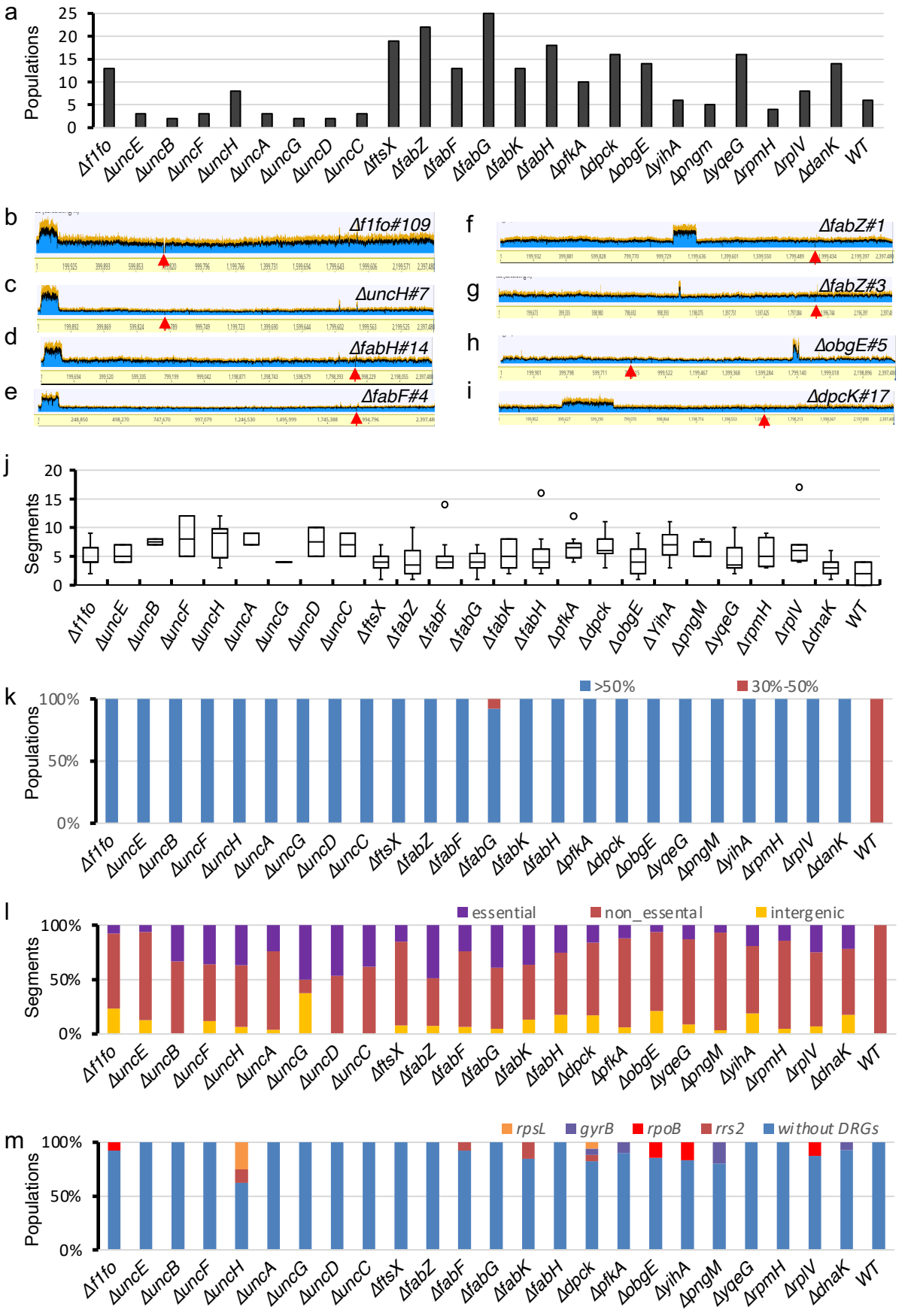
a
Populations
25
20
15
10
5
0
Δf1fo
ΔuncE
ΔuncB
ΔuncF
ΔuncH
ΔuncA
ΔuncG
ΔuncD
ΔuncC
ΔftsX
ΔfabZ
ΔfabF
ΔfabG
ΔfabK
ΔfabH
ΔpfkA
Δdpck
ΔobgE
ΔyihA
Δpngm
ΔyqeG
ΔrpmH
ΔrplV
ΔdanK
WT
b
Δf1fo#109
c
ΔuncH#7
d
ΔfabH#14
e
ΔfabF#4
f
ΔfabZ#1
g
ΔfabZ#3
h
ΔobgE#5
i
ΔdpcK#17
j
Segments
20
15
10
5
0
Δf1fo
ΔuncE
ΔuncB
ΔuncF
ΔuncH
ΔuncA
ΔuncG
ΔuncD
ΔuncC
ΔftsX
ΔfabZ
ΔfabF
ΔfabG
ΔfabK
ΔfabH
ΔpfkA
Δdpck
ΔobgE
Δ YihA
ΔpngM
ΔyqeG
ΔrpmH
ΔrplV
ΔdnaK
WT
k
>50%
30%-50%
Populations
100%
50%
0%
Δf1fo
ΔuncE
ΔuncB
ΔuncF
ΔuncH
ΔuncA
ΔuncG
ΔuncD
ΔuncC
ΔftsX
ΔfabZ
ΔfabF
ΔfabG
ΔfabK
ΔfabH
ΔpfkA
Δdpck
ΔobgE
ΔyqeG
ΔpngM
ΔyihA
ΔrpmH
ΔrplV
ΔdanK
WT
l
essential
non_essental
intergenic
Segments
100%
50%
0%
Δf1fo
ΔuncE
ΔuncB
ΔuncF
ΔuncH
ΔuncA
ΔuncG
ΔuncD
ΔuncC
ΔftsX
ΔfabZ
ΔfabF
ΔfabG
ΔfabK
ΔfabH
Δdpck
ΔpfkA
ΔobgE
ΔyqeG
ΔpngM
ΔyihA
ΔrpmH
ΔrplV
ΔdnaK
WT
m
rpsL
gyrB
rpoB
rrs2
without DRGs
Populations
100%
50%
0%
Δf1fo
ΔuncE
ΔuncB
ΔuncF
ΔuncH
ΔuncA
ΔuncG
ΔuncD
ΔuncC
ΔftsX
ΔfabZ
ΔfabF
ΔfabG
ΔfabK
ΔfabH
Δdpck
ΔpfkA
ΔobgE
ΔyihA
ΔpngM
ΔyqeG
ΔrpmH
ΔrplV
ΔdnaK
WT

Fig.3

a

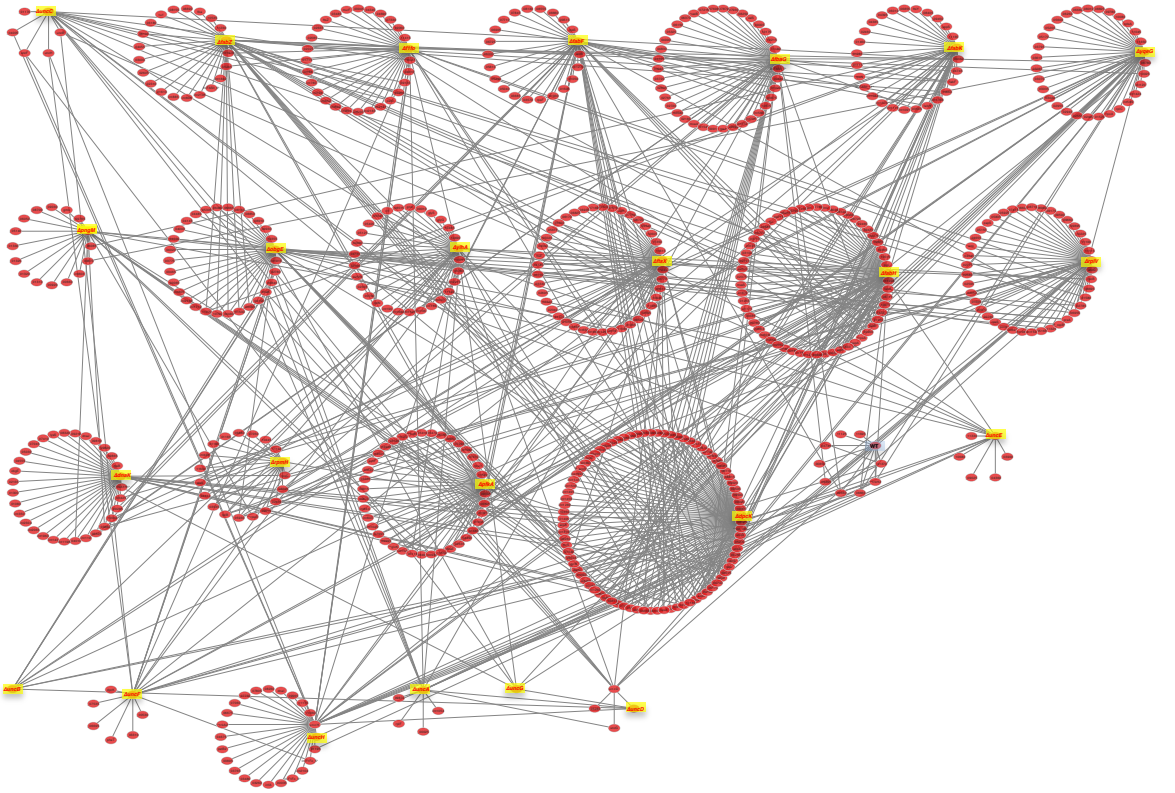

b

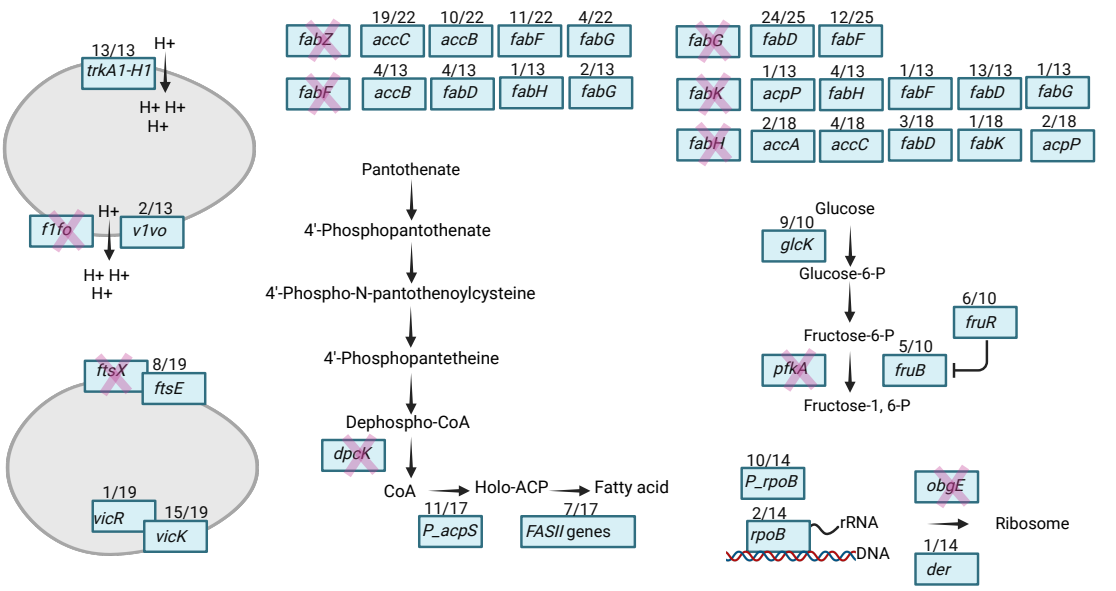
13/13
trkA1-H1
H+
H+ H+
H+
f1fo
H+
2/13
v1vo
H+ H+
H+
ftsX
8/19
ftsE
1/19
vicR
15/19
vicK
19/22
fabZ
accC
10/22
accB
11/22
fabF
4/22
fabG
fabF
4/13
accB
4/13
fabD
1/13
fabH
2/13
fabG
Pantothenate
4'-Phosphopantothenate
4'-Phospho-N-pantothenoylcysteine
4'-Phosphopantetheine
Dephospho-CoA
dpcK
CoA
Holo-ACP
Fatty acid
11/17
P_acpS
7/17
FASII genes
24/25
fabG
fabD
12/25
fabF
fabK
1/13
acpP
4/13
fabH
1/13
fabF
13/13
fabD
1/13
fabG
fabH
2/18
accA
4/18
accC
3/18
fabD
1/18
fabK
2/18
acpP
Glucose
9/10
glcK
Glucose-6-P
6/10
fruR
Fructose-6-P
5/10
fruB
pfkA
Fructose-1, 6-P
10/14
P_rpoB
2/14
rpoB
rRNA
DNA
obgE
Ribosome
1/14
der

Fig.4

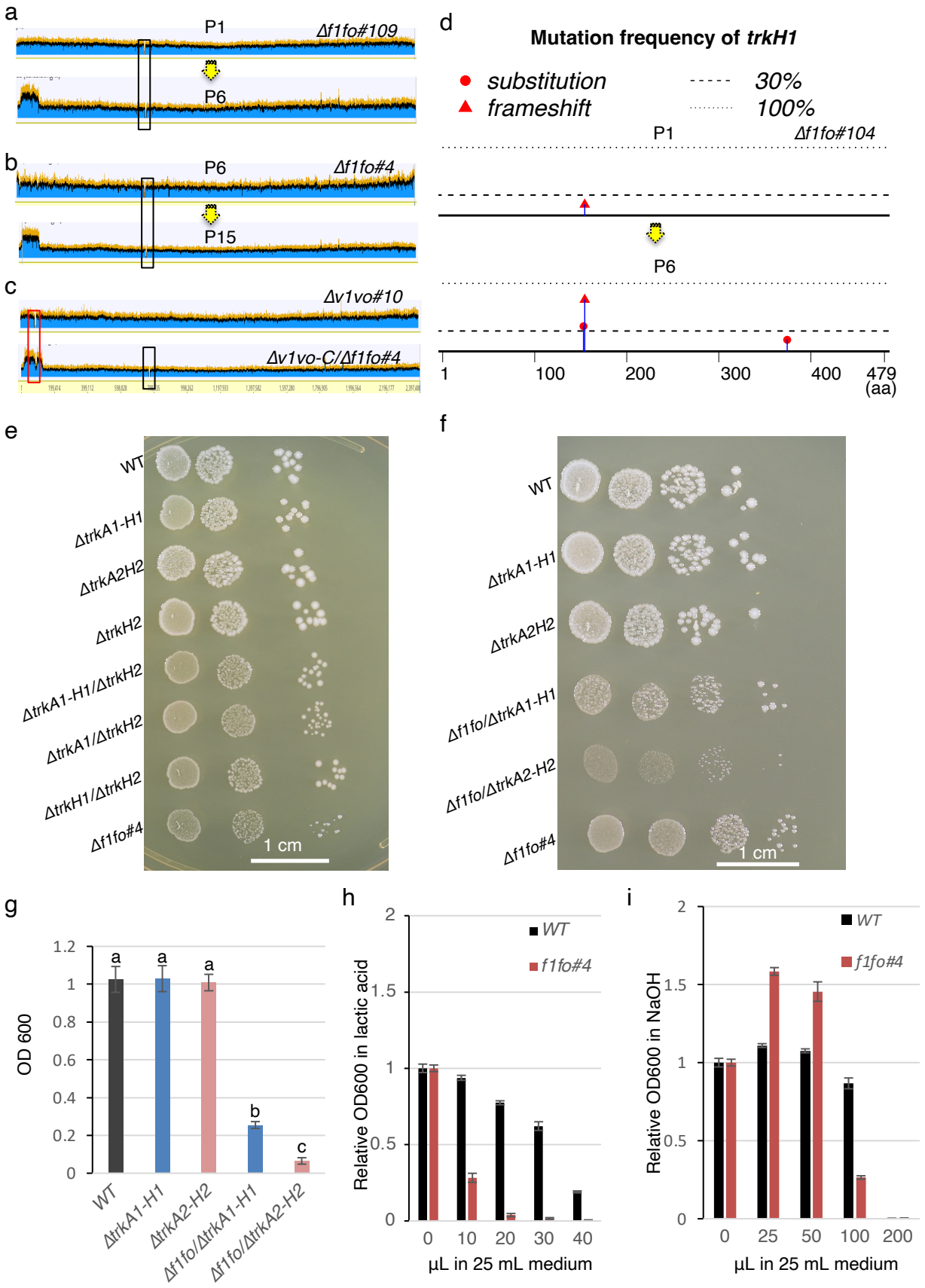
a
P1
Δf1fo#109
P6
b
P6
Δf1fo#4
P15
c
Δv1vo#10
Δv1vo-C/Δf1fo#4
d
Mutation frequency of trkH1
substitution
frameshift
30%
100%
P1
Δf1fo#104
P6
1
100
200
300
400
479
(aa)
e
WT
ΔtrkA1-H1
ΔtrkA2H2
ΔtrkH2
ΔtrkA1-H1/ΔtrkH2
ΔtrkA1/ΔtrkH2
ΔtrkH1/ΔtrkH2
Δf1fo#4
1 cm
f
WT
ΔtrkA1-H1
ΔtrkA2H2
Δf1fo/ΔtrkA1-H1
Δf1fo/ΔtrkA2-H2
Δf1fo#4
1 cm
g
OD 600
1.2
1
0.8
0.6
0.4
0.2
0
a
a
a
b
c
WT
ΔtrkA1-H1
ΔtrkA2-H2
Δf1fo/ΔtrkA1-H1
Δf1fo/ΔtrkA2-H2
h
Relative OD600 in lactic acid
2
1.5
1
0.5
0
WT
f1fo#4
0
10
20
30
40
μL in 25 mL medium
i
Relative OD600 in NaOH
2
1.5
1
0.5
0
WT
f1fo#4
0
25
50
100
200
μL in 25 mL medium

Fig.5

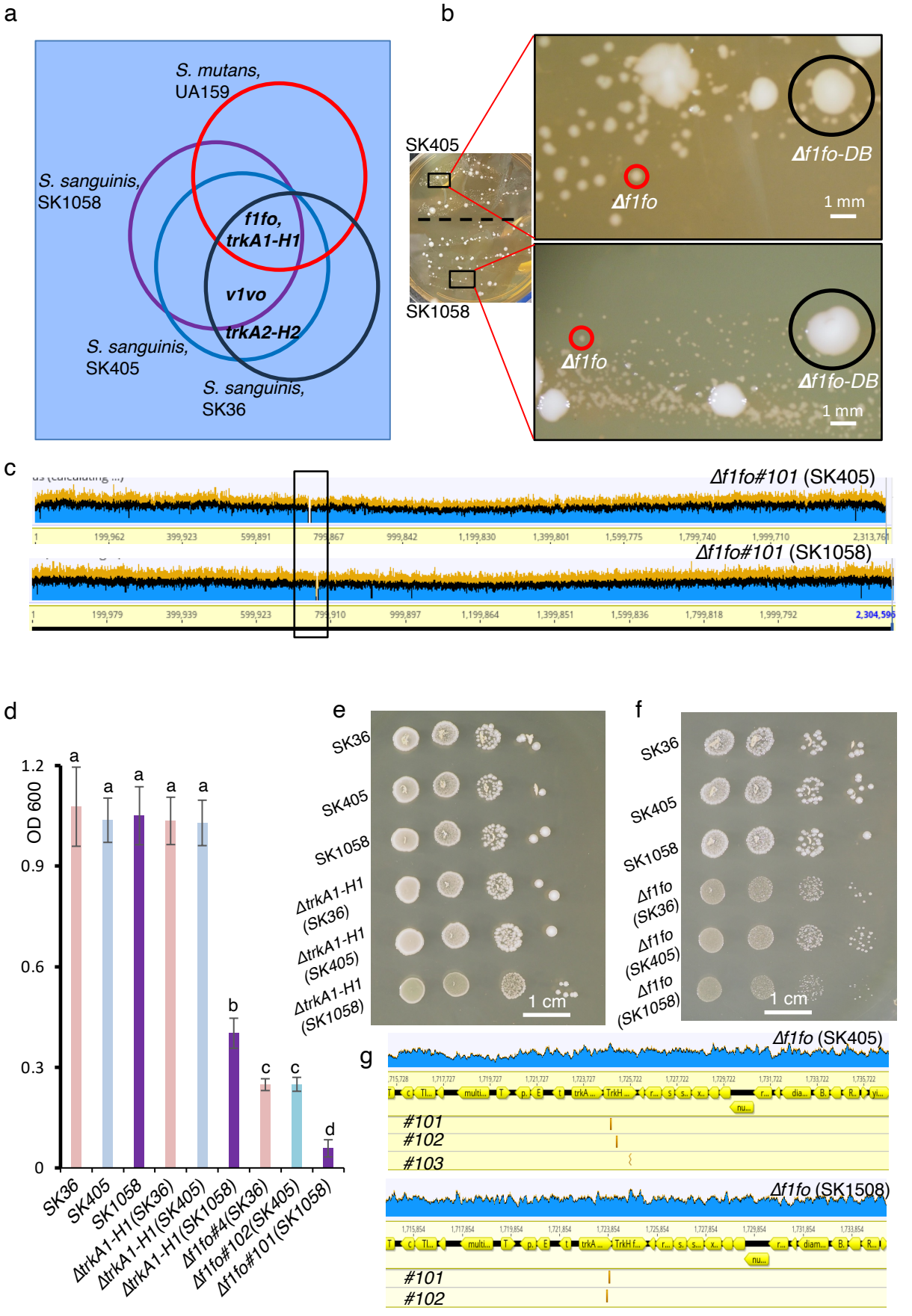
a
S. mutans, UA159
S. sanguinis, SK1058
f1fo, trkA1-H1
v1vo
trkA2-H2
S. sanguinis, SK405
S. sanguinis, SK36
b
SK405
SK1058
Δf1fo-DB
Δf1fo
1 mm
c
Δf1fo#101 (SK405)
Δf1fo#101 (SK1058)
d
OD 600
SK36
SK405
SK1058
ΔtrkA1-H1(SK36)
ΔtrkA1-H1(SK405)
ΔtrkA1-H1(SK1058)
Δf1fo#4(SK36)
Δf1fo#102(SK405)
Δf1fo#101(SK1058)
e
1 cm
f
1 cm
g
Δf1fo (SK405)
#101
#102
#103
Δf1fo (SK1508)
#101
#102

Fig S1

a

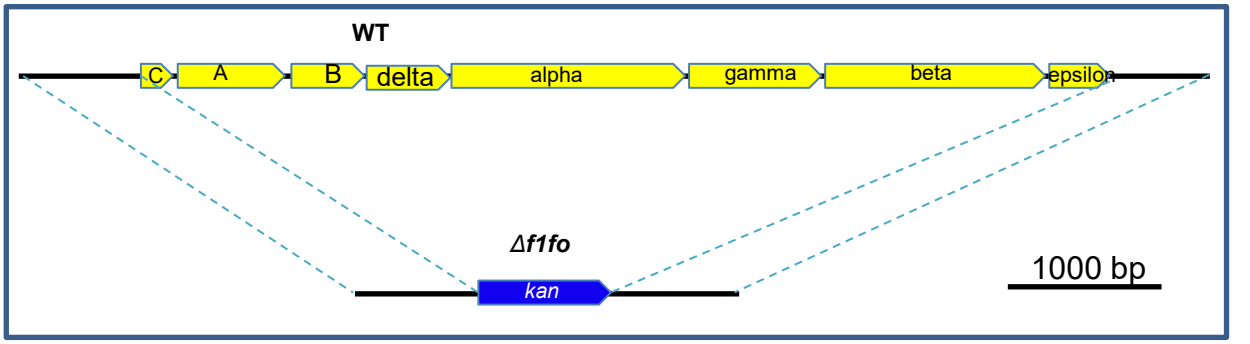
WT
C
A
B
delta
alpha
gamma
beta
epsilon
Δf1fo
kan
1000 bp

b

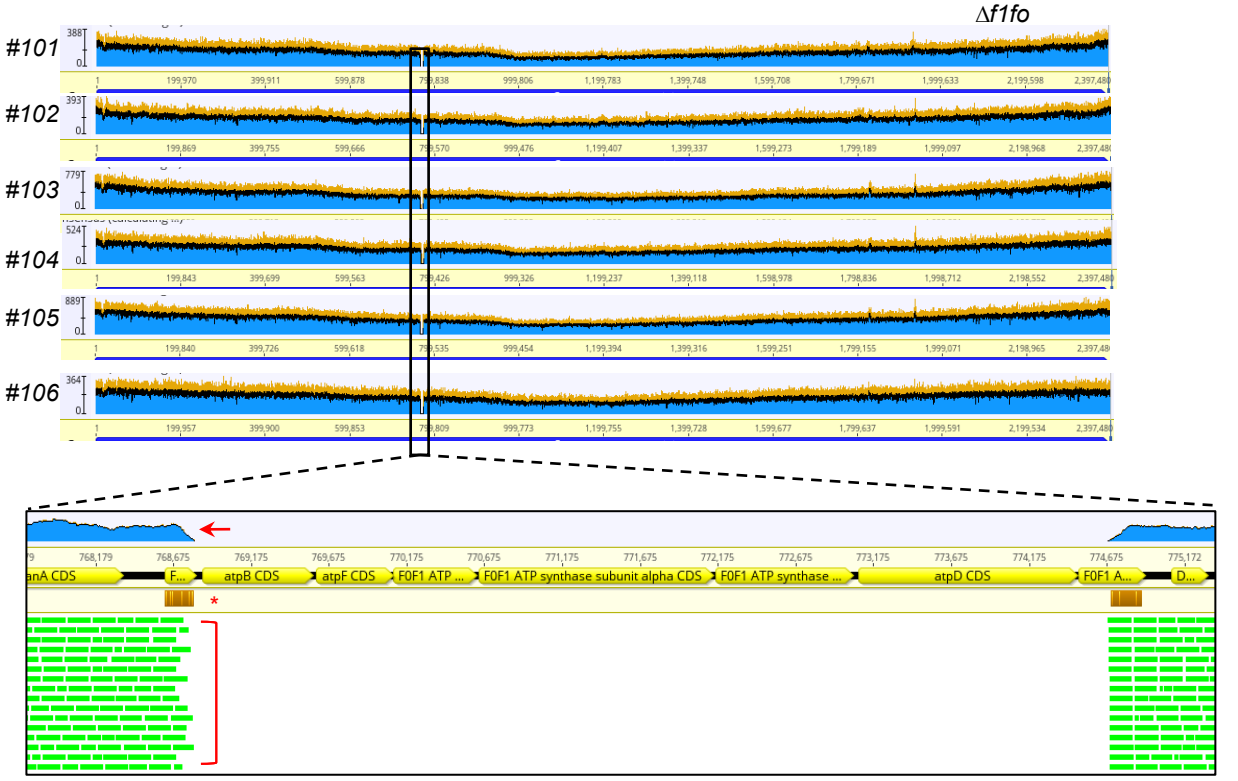
Δf1fo
#101
#102
#103
#104
#105
#106
anA CDS
F...
atpB CDS
atpF CDS
F0F1 ATP ...
F0F1 ATP synthase subunit alpha CDS
F0F1 ATP synthase ...
atpD CDS
F0F1 A...
D...
*

c

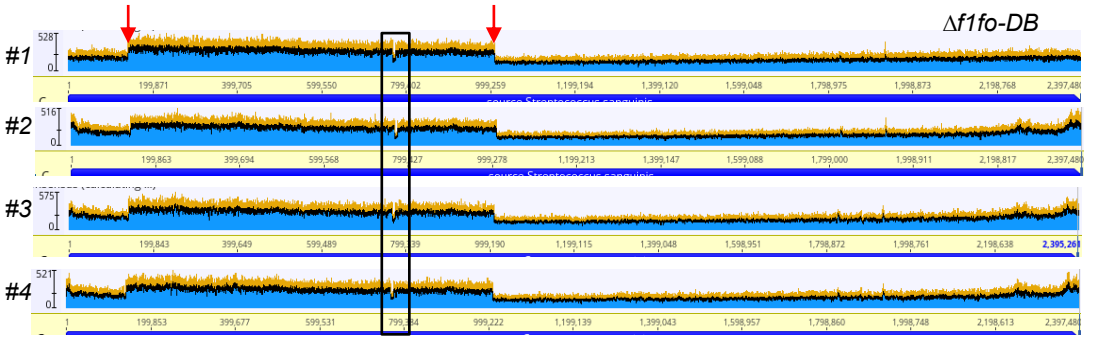
Δf1fo-DB
#1
#2
#3
#4

Fig.S2

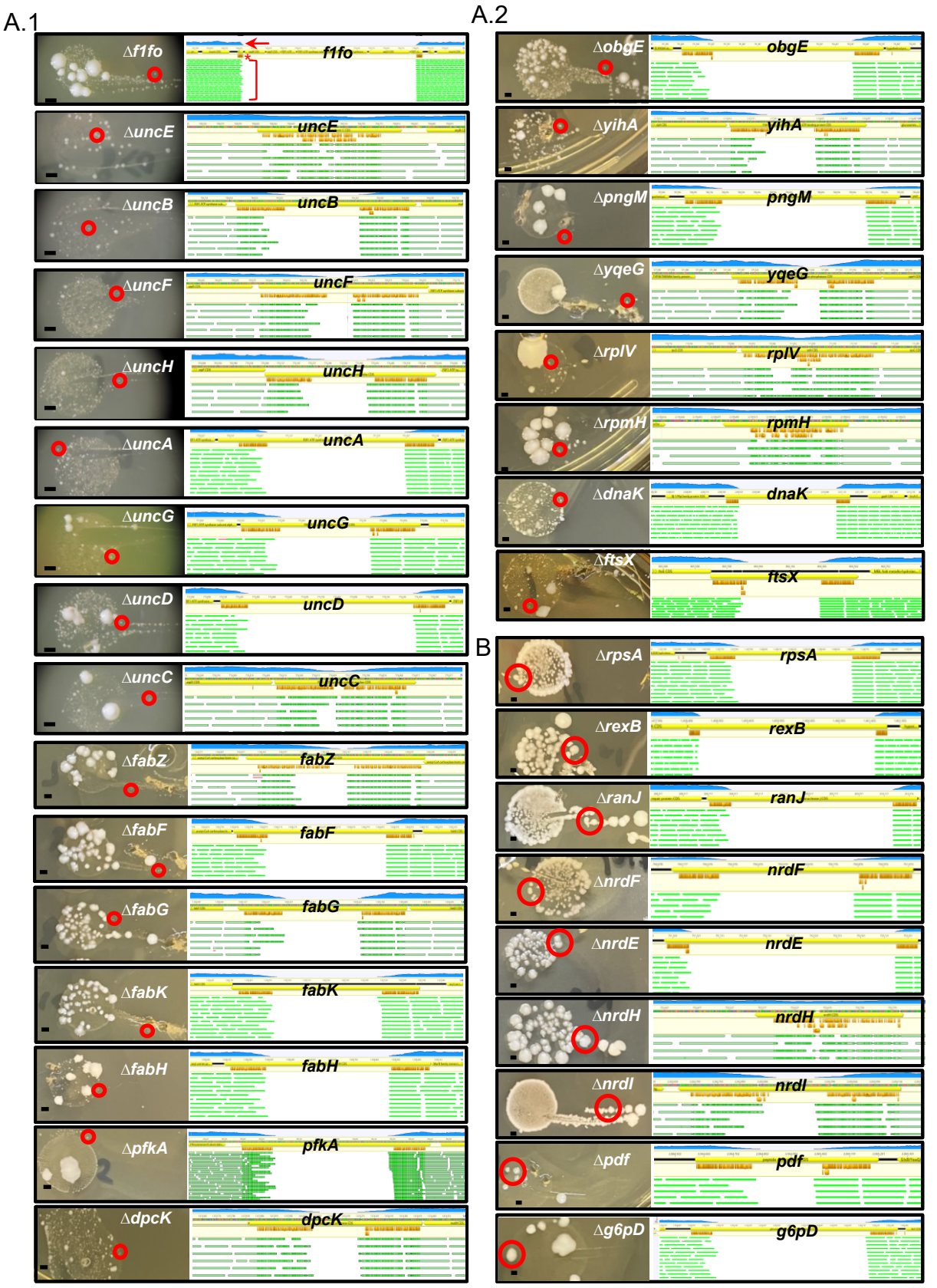
A.1
Δf1fo
f1fo
ΔuncE
uncE
ΔuncB
uncB
ΔuncF
uncF
ΔuncH
uncH
ΔuncA
uncA
ΔuncG
uncG
ΔuncD
uncD
ΔuncC
uncC
ΔfabZ
fabZ
ΔfabF
fabF
ΔfabG
fabG
ΔfabK
fabK
ΔfabH
fabH
ΔpfkA
pfkA
ΔdpcK
dpcK
A.2
ΔobgE
obgE
ΔyihA
yihA
ΔpngM
pngM
ΔyqeG
yqeG
ΔrplV
rplV
ΔrpmH
rpmH
ΔdnaK
dnaK
ΔftsX
ftsX
B
ΔrpsA
rpsA
ΔrexB
rexB
ΔranJ
ranJ
ΔnrdF
nrdF
ΔnrdE
nrdE
ΔnrdH
nrdH
ΔnrdI
nrdI
Δpdf
pdf
Δg6pD
g6pD

Fig S3

a

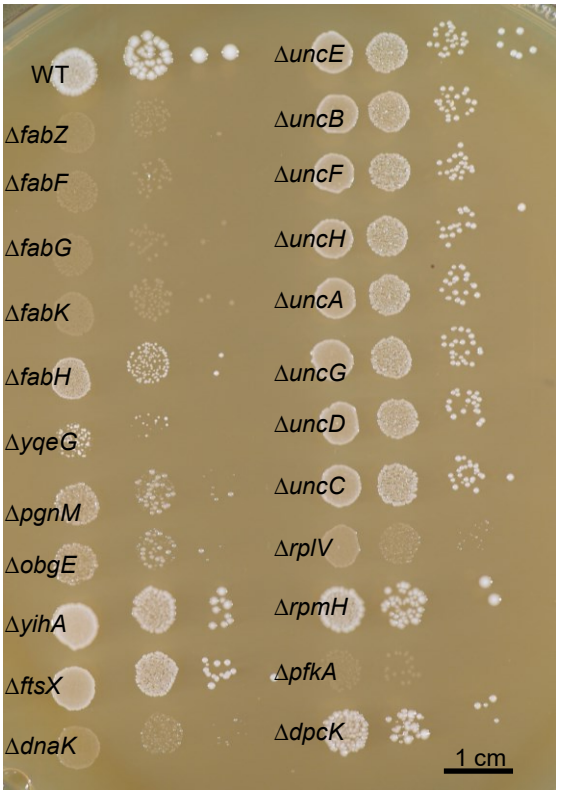
WT
ΔfabZ
ΔfabF
ΔfabG
ΔfabK
ΔfabH
ΔyqeG
ΔpgnM
ΔobgE
ΔyihA
ΔftsX
ΔdnaK
ΔuncE
ΔuncB
ΔuncF
ΔuncH
ΔuncA
ΔuncG
ΔuncD
ΔuncC
ΔrplV
ΔrpmH
ΔpfkA
ΔdpcK
1 cm

b

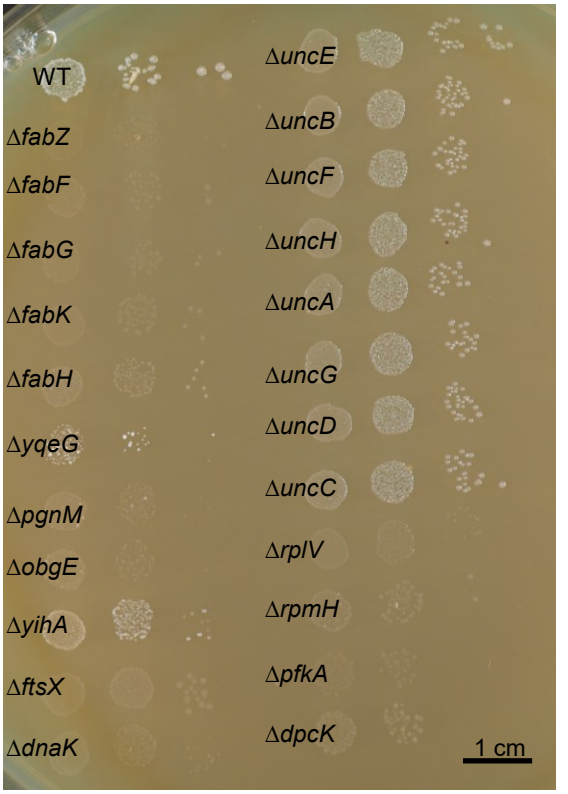
WT
ΔfabZ
ΔfabF
ΔfabG
ΔfabK
ΔfabH
ΔyqeG
ΔpgnM
ΔobgE
ΔyihA
ΔftsX
ΔdnaK
ΔuncE
ΔuncB
ΔuncF
ΔuncH
ΔuncA
ΔuncG
ΔuncD
ΔuncC
ΔrplV
ΔrpmH
ΔpfkA
ΔdpcK
1 cm

c

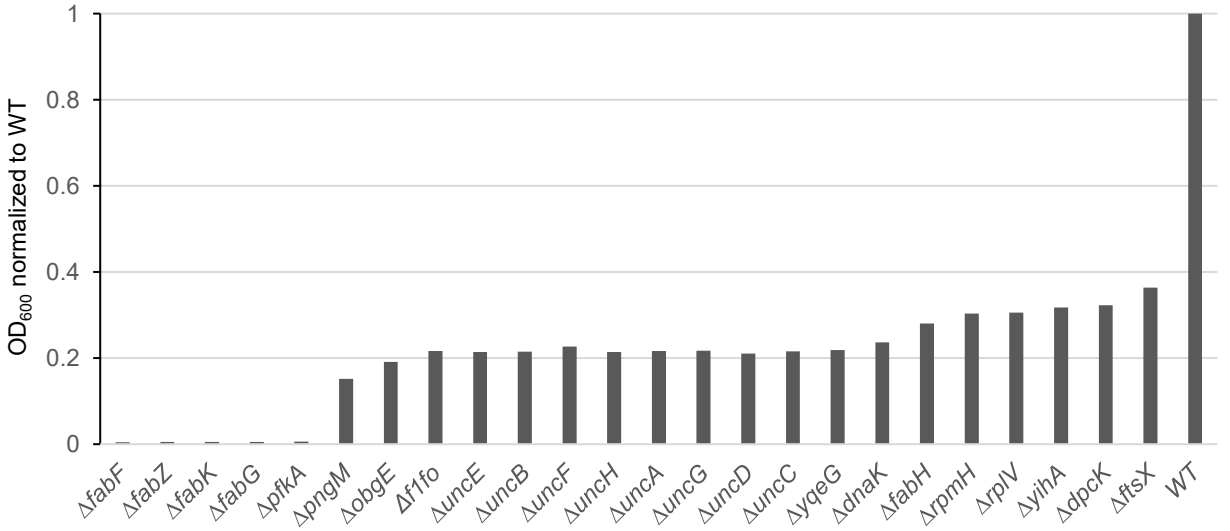
OD600 normalized to WT
1
0.8
0.6
0.4
0.2
0
ΔfabF
ΔfabZ
ΔfabK
ΔfabG
ΔpfkA
ΔpngM
ΔobgE
Δf1fo
ΔuncE
ΔuncB
ΔuncF
ΔuncH
ΔuncA
ΔuncG
ΔuncD
ΔuncC
ΔyqeG
ΔdnaK
ΔfabH
ΔrpmH
ΔrplV
ΔyihA
ΔdpcK
ΔftsX
WT

Fig S4

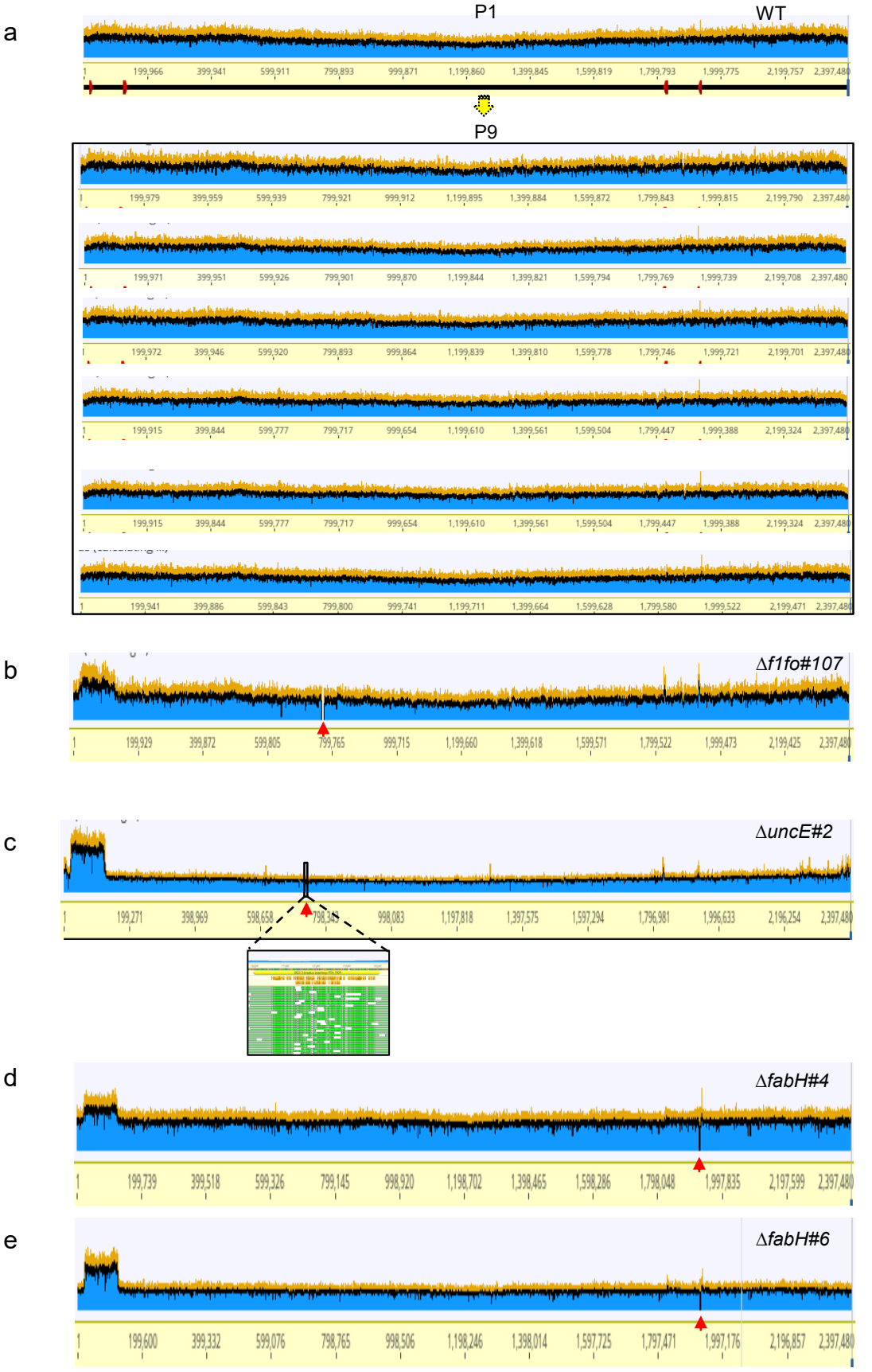

Fig S5

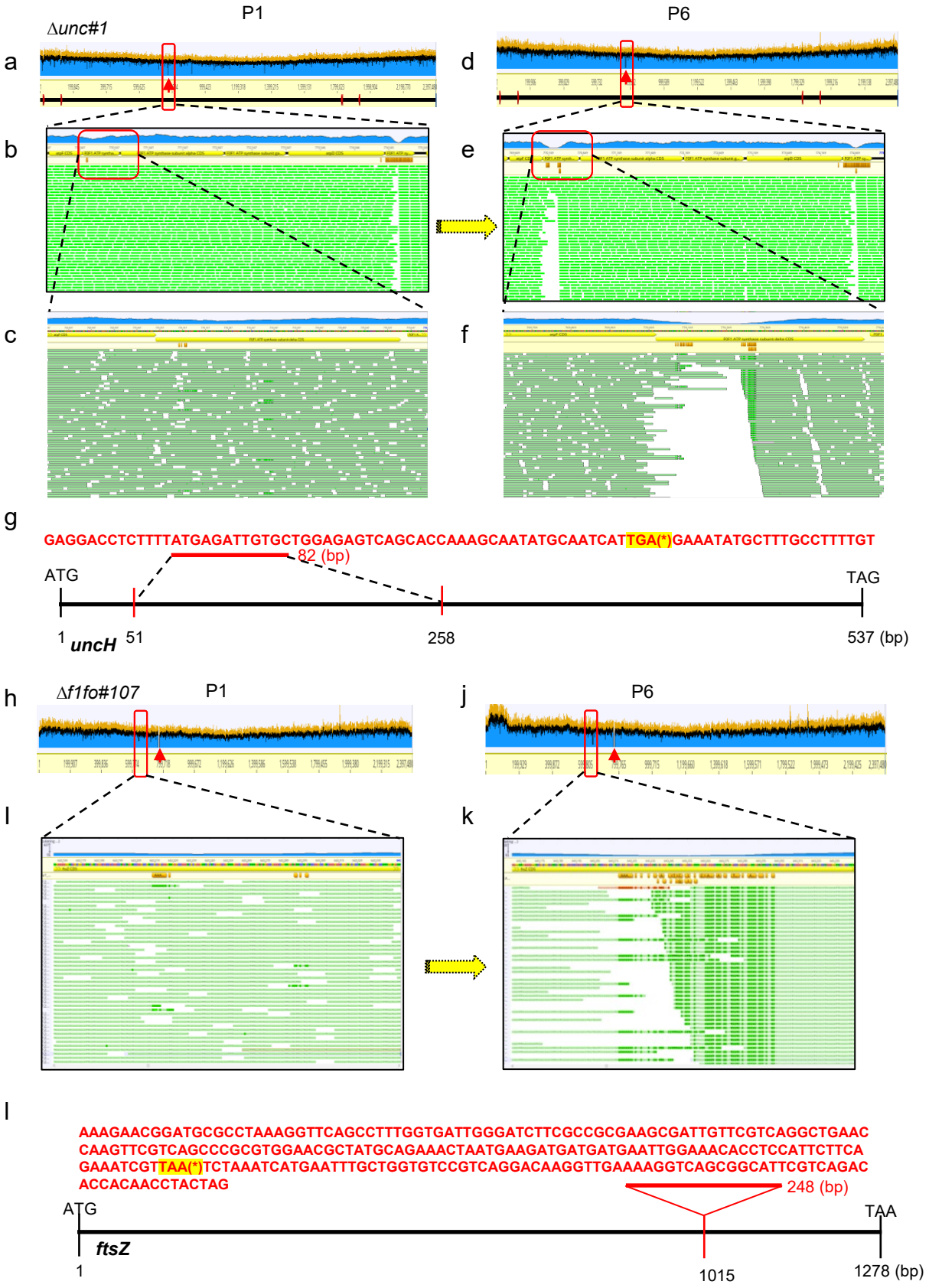
P1
P6
Δunc#1
a
b
c
d
e
f
g
GAGGACCTCTTTTATGAGATTGTGCTGGAGAGTCAGCACCAAAGCAATATGCAATCATTGA(*)GAAATATGCTTTGCCTTTTGT
82 (bp)
ATG
TAG
1
uncH
51
258
537 (bp)
Δf1fo#107
P1
P6
h
j
l
k
l
AAAGAACGGATGCGCCTAAAGGTTCAGCCTTTGGTGATTGGGATCTTCGCCGCGAAGCGATTGTTCGTCAGGCTGAAC
CAAGTTCGTCAGCCCGCGTGGAACGCTATGCAGAAACTAATGAAGATGATGATGAATTGGAAACACCTCCATTCTTCA
GAAATCGTTAA(*)TCTAAATCATGAATTTGCTGGTGTCCGTCAGGACAAGGTTGAAAAGGTCAGCGGCATTCGTCAGAC
ACCACAACCTACTAG
248 (bp)
ATG
TAA
ftsZ
1
1015
1278 (bp)

Fig S6

a

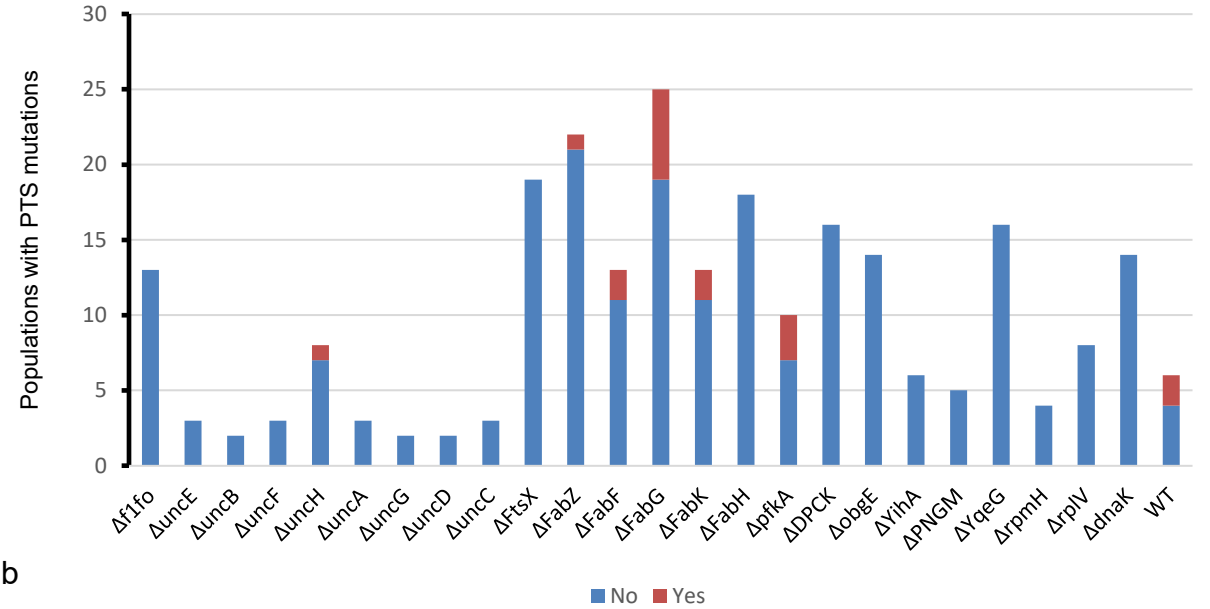
Populations with PTS mutations
30
25
20
15
10
5
0
Δf1fo
ΔuncE
ΔuncB
ΔuncF
ΔuncH
ΔuncA
ΔuncG
ΔuncD
ΔuncC
ΔFtsX
ΔFabZ
ΔFabF
ΔFabG
ΔFabK
ΔFabH
ΔpfkA
ΔDPCK
ΔobgE
ΔYihA
ΔPNGM
ΔYqeG
ΔrpmH
ΔrplV
ΔdnaK
WT
No
Yes

b

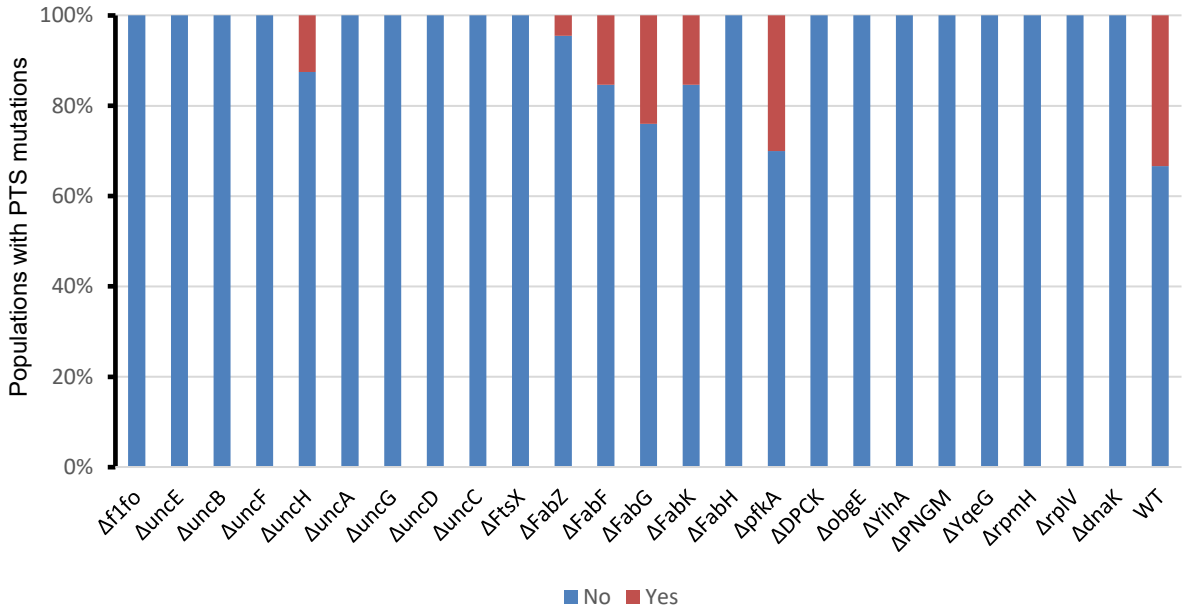
Populations with PTS mutations
100%
80%
60%
40%
20%
0%
Δf1fo
ΔuncE
ΔuncB
ΔuncF
ΔuncH
ΔuncA
ΔuncG
ΔuncD
ΔuncC
ΔFtsX
ΔFabZ
ΔFabF
ΔFabG
ΔFabK
ΔFabH
ΔpfkA
ΔDPCK
ΔobgE
ΔYihA
ΔPNGM
ΔYqeG
ΔrpmH
ΔrplV
ΔdnaK
WT
No
Yes

Fig S7

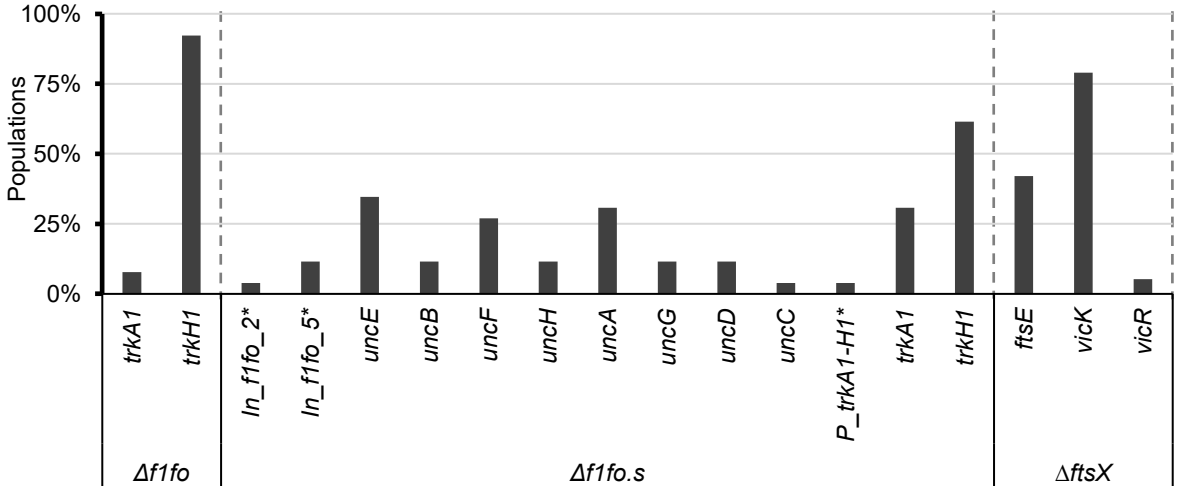
100%
75%
50%
25%
0%
Populations
trkA1
trkH1
In_f1fo_2*
In_f1fo_5*
uncE
uncB
uncF
uncH
uncA
uncG
uncD
uncC
P_trkA1-H1*
trkA1
trkH1
ftsE
vicK
vicR
Δf1fo
Δf1fo.s
ΔftsX

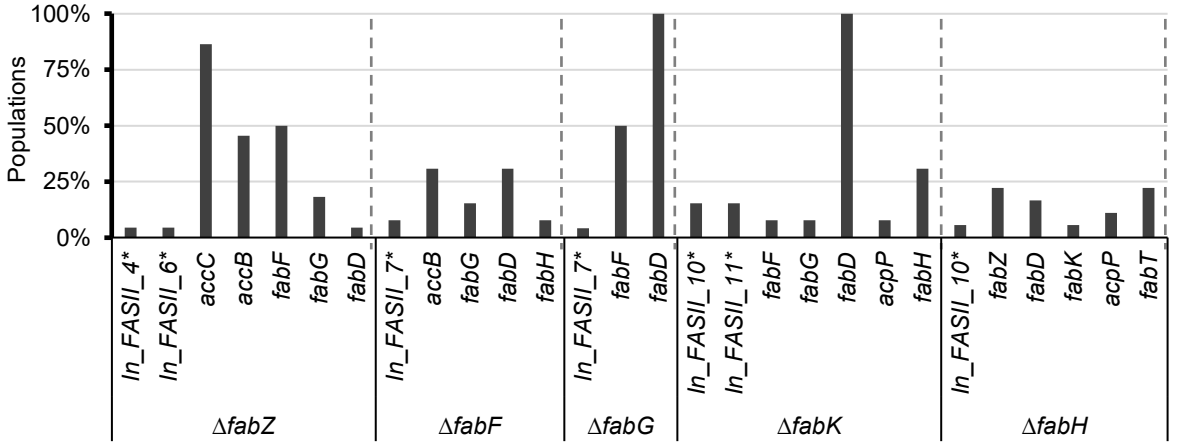
100%
75%
50%
25%
0%
Populations
In_FASII_4*
In_FASII_6*
accC
accB
fabF
fabG
fabD
In_FASII_7*
accB
fabG
fabD
fabH
In_FASII_7*
fabF
fabD
In_FASII_10*
In_FASII_11*
fabF
fabG
fabD
acpP
fabH
In_FASII_10*
fabZ
fabD
fabK
acpP
fabT
ΔfabZ
ΔfabF
ΔfabG
ΔfabK
ΔfabH

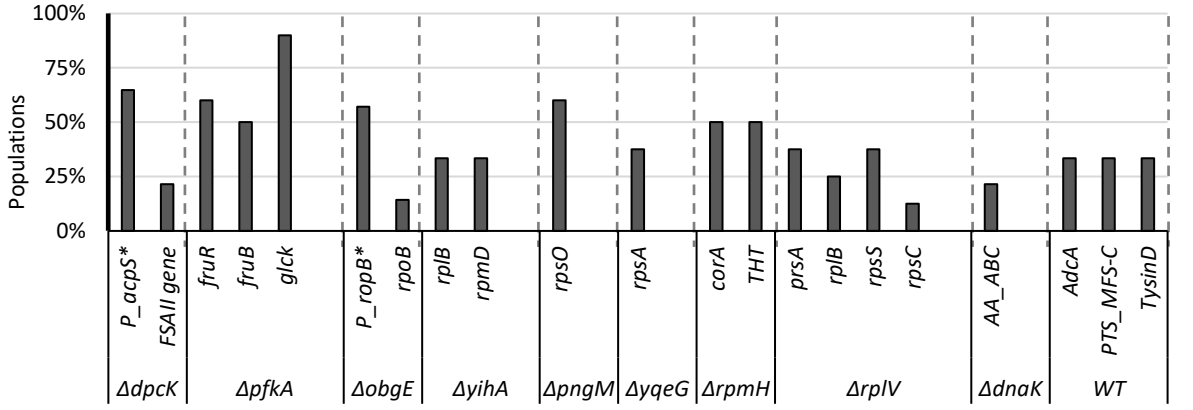
100%
75%
50%
25%
0%
Populations
P_acpS*
FSAII gene
fruR
fruB
glck
P_ropB*
rpoB
rplB
rpmD
rpsO
rpsA
corA
THT
prsA
rplB
rpsS
rpsC
AA_ABC
AdcA
PTS_MFS-C
TysinD
ΔdpcK
ΔpfkA
ΔobgE
ΔyihA
ΔpngM
ΔyqeG
ΔrpmH
ΔrplV
ΔdnaK
WT

Fig S8

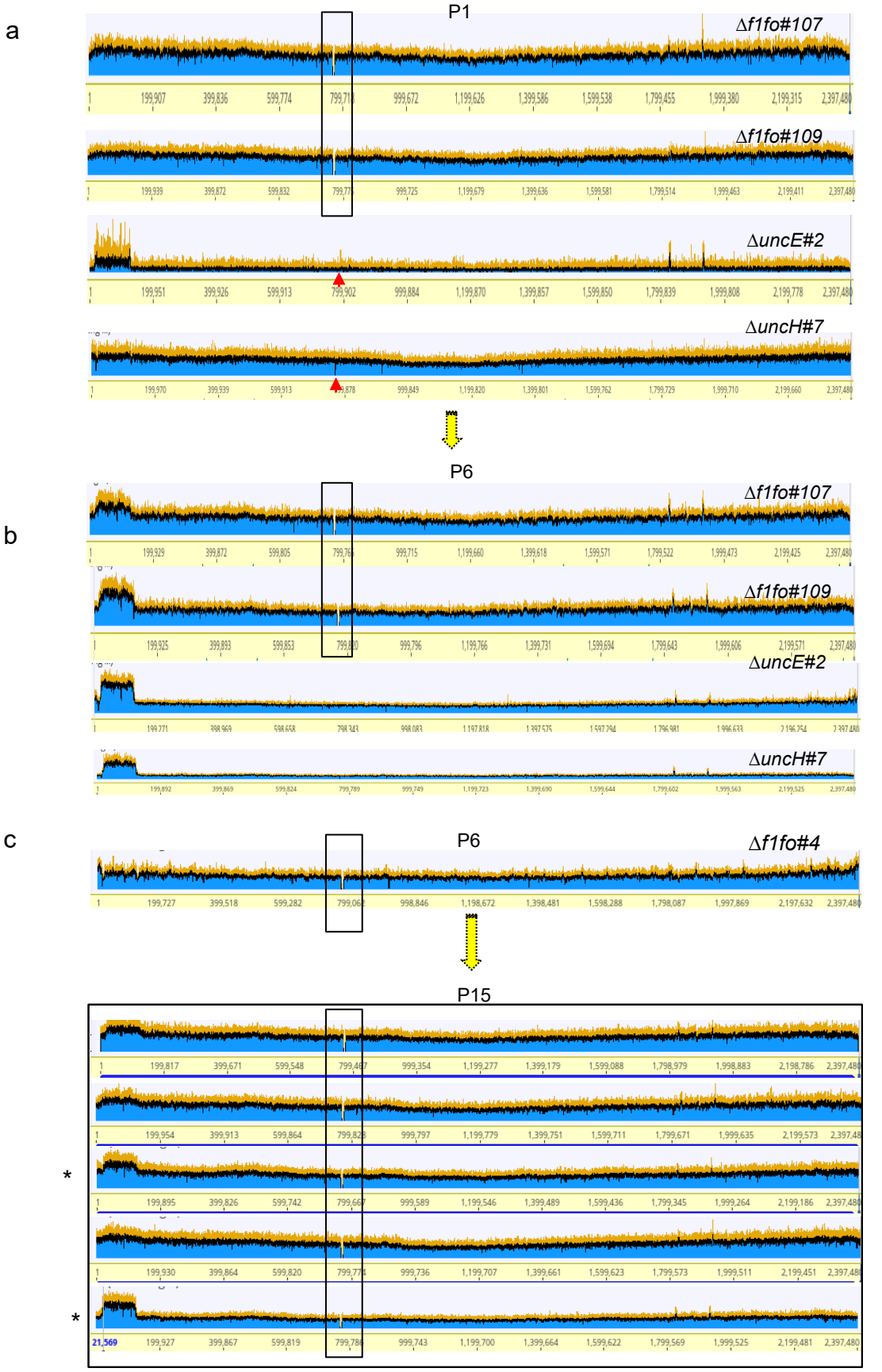
a
P1
Δf1fo#107
Δf1fo#109
ΔuncE#2
ΔuncH#7
b
P6
Δf1fo#107
Δf1fo#109
ΔuncE#2
ΔuncH#7
c
P6
Δf1fo#4
P15
*
*

Fig S9

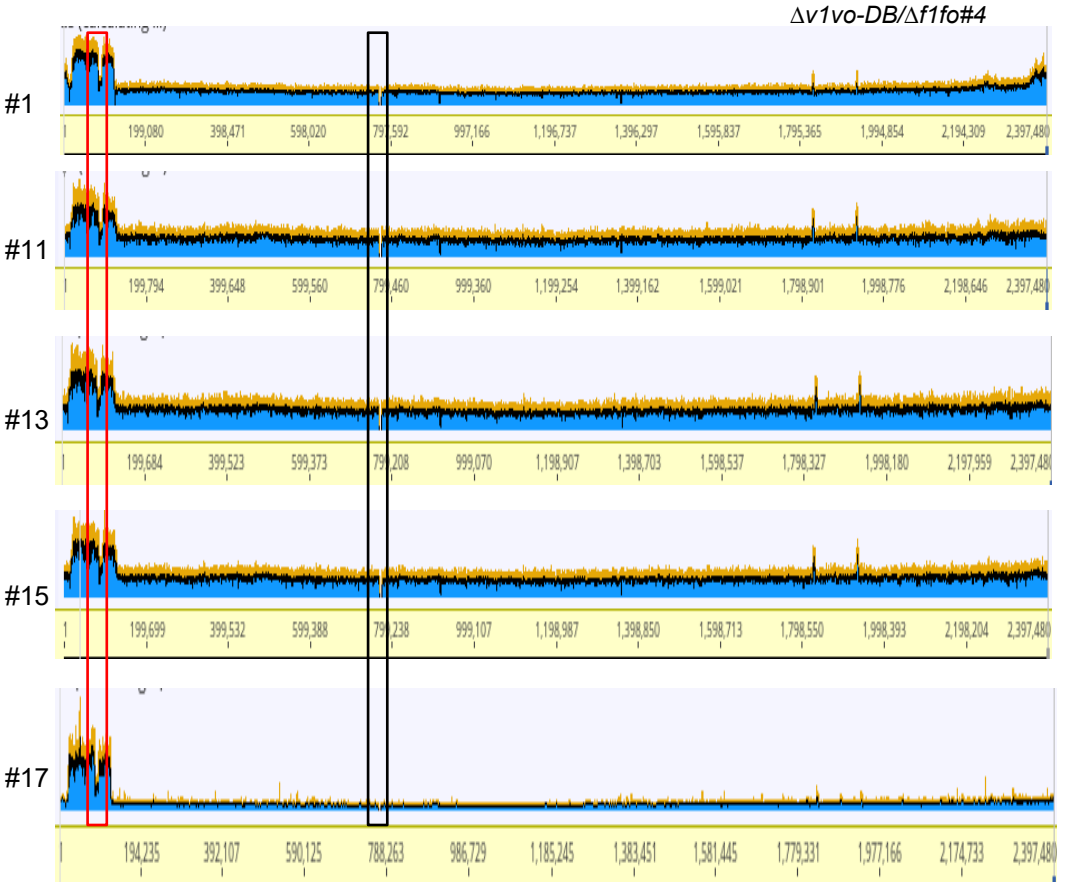
Δv1vo-DB/Δf1fo#4
#1
199,080
398,471
598,020
997,166
1,196,737
1,396,297
1,595,837
1,795,365
1,994,854
2,194,309
#11
199,794
399,648
599,560
999,360
1,199,254
1,399,162
1,599,021
1,798,901
1,998,776
2,198,646
#13
199,684
399,523
599,373
999,070
1,198,907
1,398,703
1,598,537
1,798,327
1,998,180
2,197,959
#15
199,699
399,532
599,388
999,107
1,198,987
1,398,850
1,598,713
1,798,550
1,998,393
2,198,204
#17
194,235
392,107
590,125
788,263
986,729
1,185,245
1,383,451
1,581,445
1,779,331
1,977,166
2,174,733

Fig S10

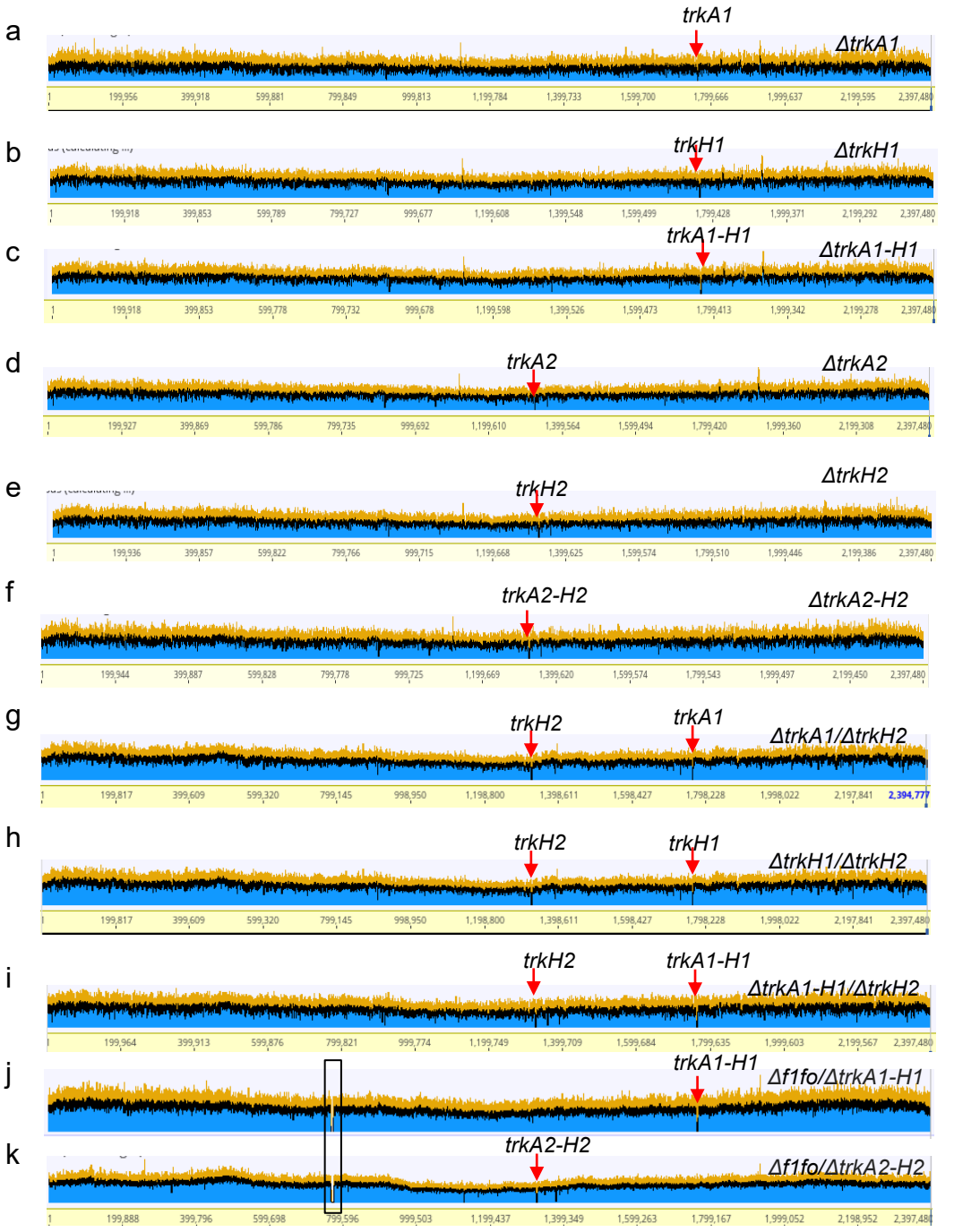
a
trkA1
ΔtrkA1
b
trkH1
ΔtrkH1
c
trkA1-H1
ΔtrkA1-H1
d
trkA2
ΔtrkA2
e
trkH2
ΔtrkH2
f
trkA2-H2
ΔtrkA2-H2
g
trkH2
trkA1
ΔtrkA1/ΔtrkH2
h
trkH2
trkH1
ΔtrkH1/ΔtrkH2
i
trkH2
trkA1-H1
ΔtrkA1-H1/ΔtrkH2
j
trkA1-H1
Δf1fo/ΔtrkA1-H1
k
trkA2-H2
Δf1fo/ΔtrkA2-H2

Fig S11 Working model for F1Fo, V1Vo, TrkA1-H1 and TrkA2-H2

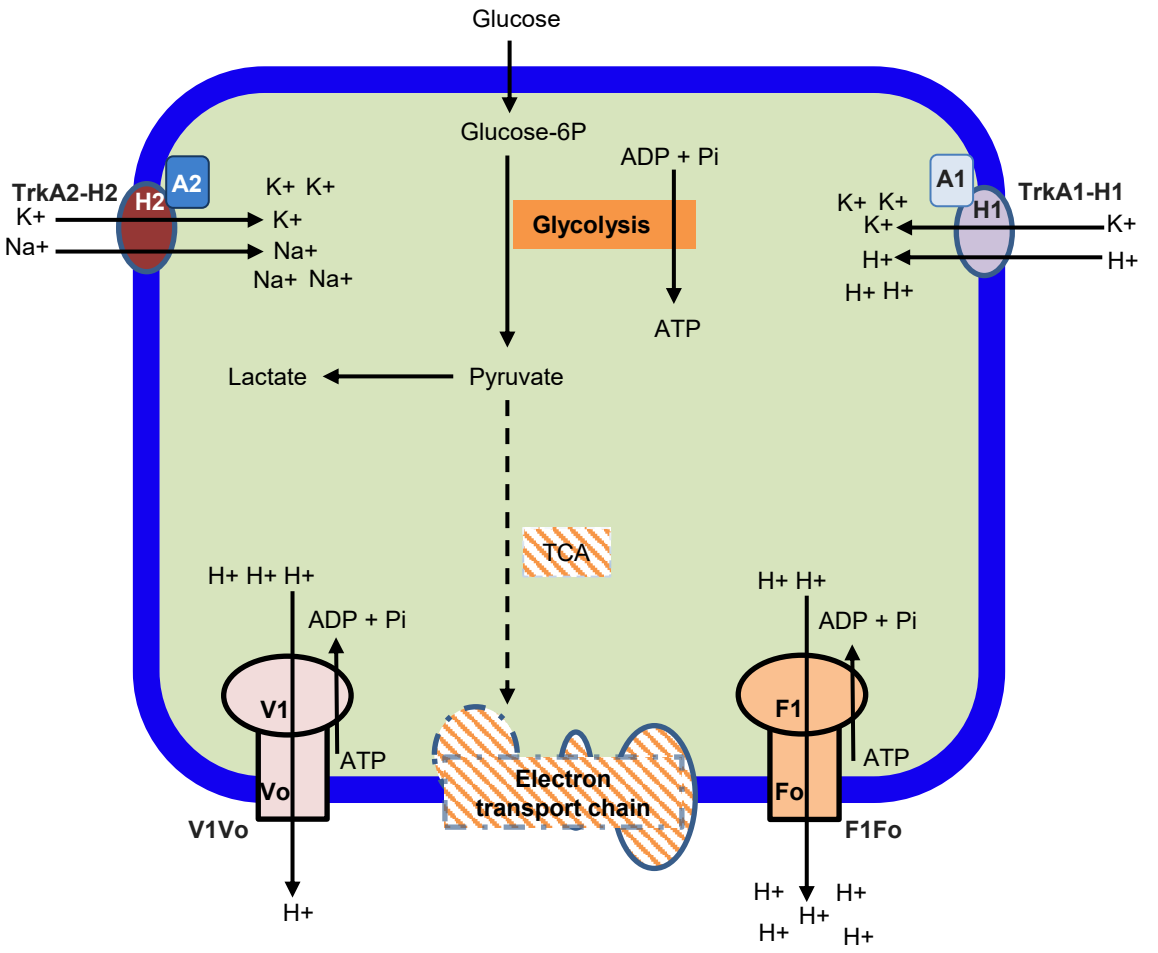

Fig S12

a

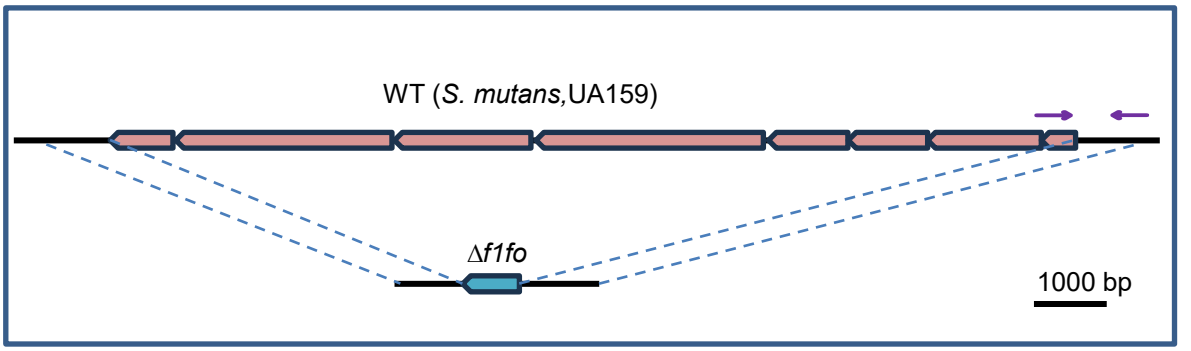

b

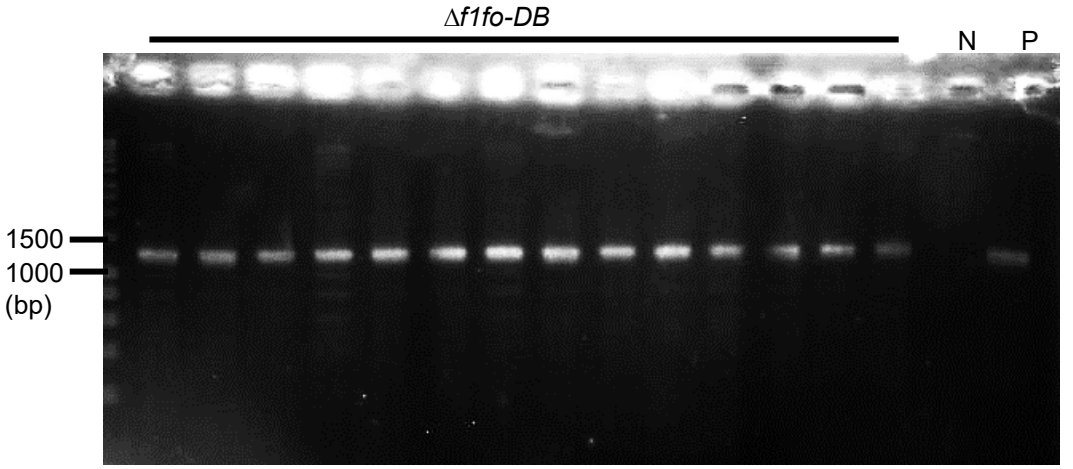

Fig S13

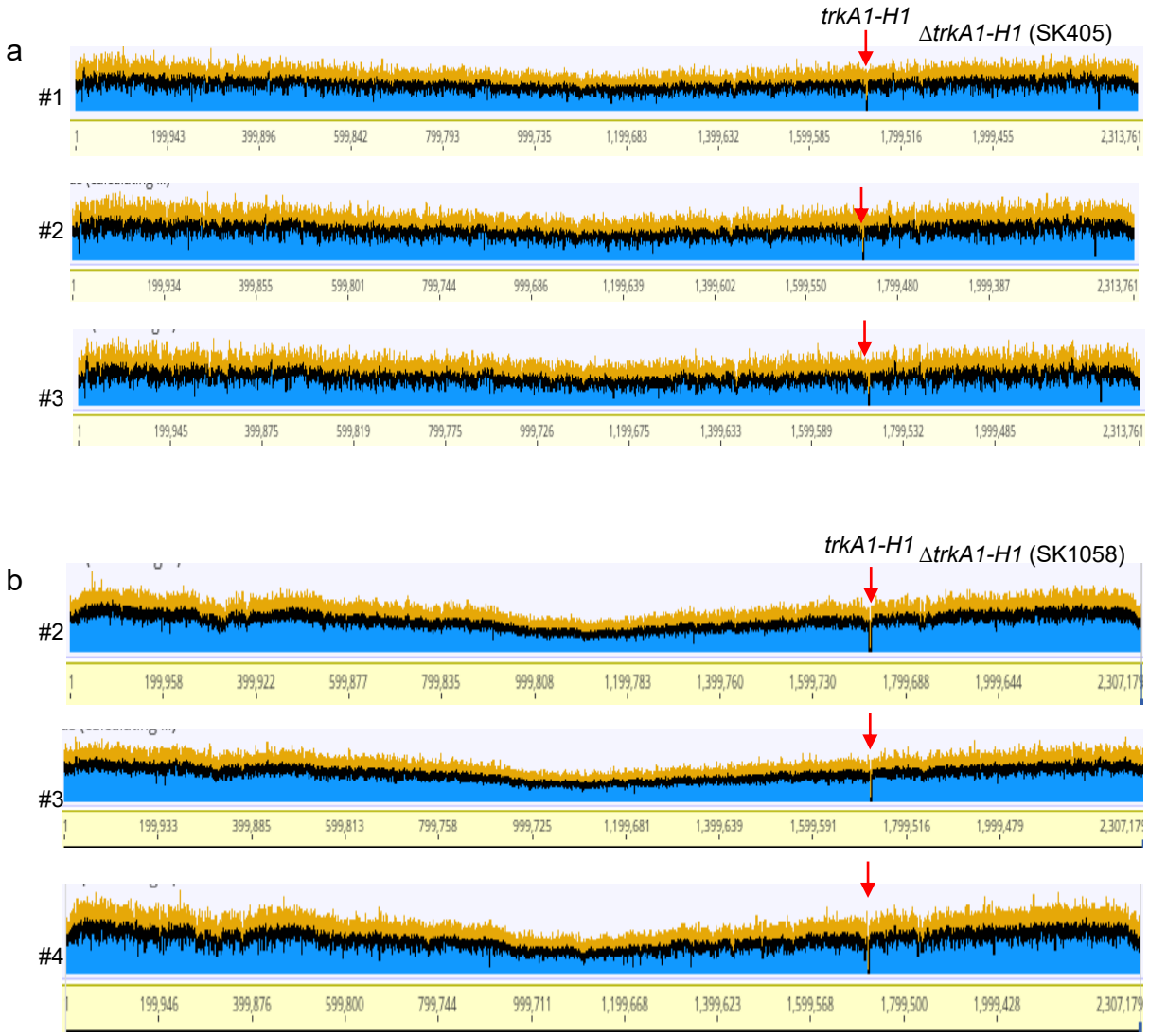
a
trkA1-H1
ΔtrkA1-H1 (SK405)
#1
1
199,943
399,896
599,842
799,793
999,735
1,199,683
1,399,632
1,599,585
1,799,516
1,999,455
2,313,761
#2
1
199,934
399,855
599,801
799,744
999,686
1,199,639
1,399,602
1,599,550
1,799,480
1,999,387
2,313,761
#3
1
199,945
399,875
599,819
799,775
999,726
1,199,675
1,399,633
1,599,589
1,799,532
1,999,485
2,313,761
b
trkA1-H1
ΔtrkA1-H1 (SK1058)
#2
1
199,958
399,922
599,877
799,835
999,808
1,199,783
1,399,760
1,599,730
1,799,688
1,999,644
#3
1
199,933
399,885
599,813
799,758
999,725
1,199,681
1,399,639
1,599,591
1,799,516
1,999,479
#4
1
199,946
399,876
599,800
799,744
999,711
1,199,668
1,399,623
1,599,568
1,799,500
1,999,428

Fig S14

a

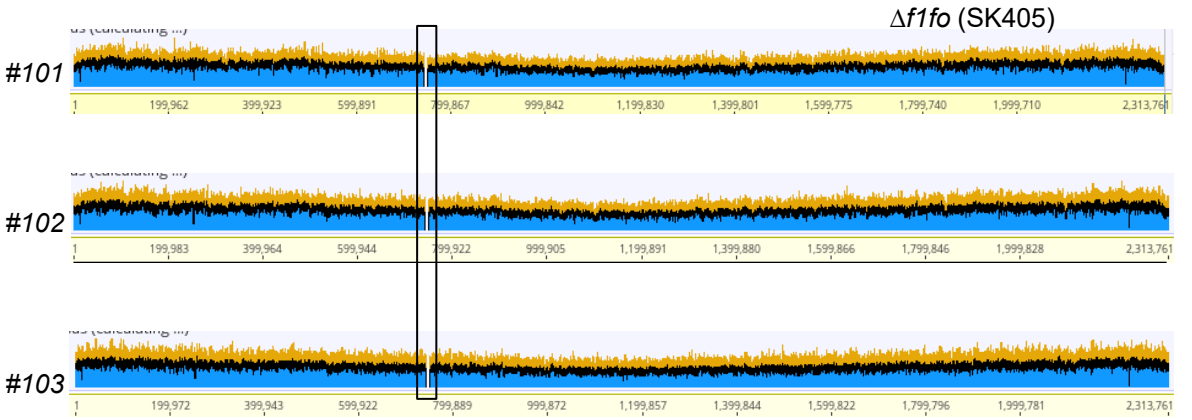
Δf1fo (SK405)
#101
1
199,962
399,923
599,891
799,867
999,842
1,199,830
1,399,801
1,599,775
1,799,740
1,999,710
2,313,761
#102
1
199,983
399,964
599,944
799,922
999,905
1,199,891
1,399,880
1,599,866
1,799,846
1,999,828
2,313,761
#103
1
199,972
399,943
599,922
799,889
999,872
1,199,857
1,399,844
1,599,822
1,799,796
1,999,781
2,313,761

b

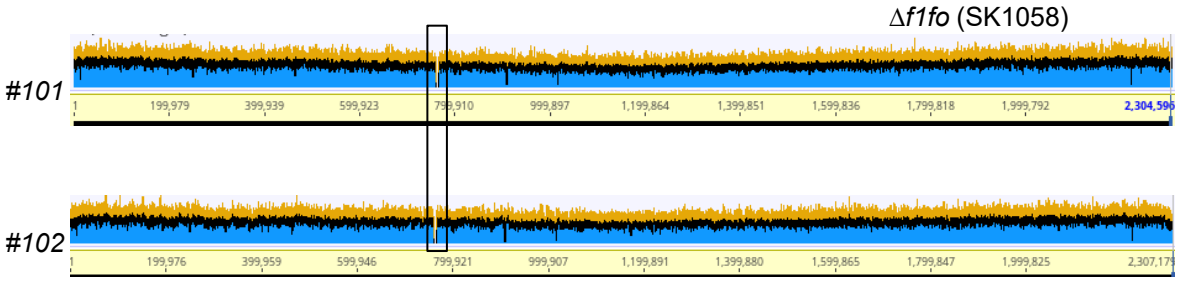
Δf1fo (SK1058)
#101
1
199,979
399,939
599,923
799,910
999,897
1,199,864
1,399,851
1,599,836
1,799,818
1,999,792
2,304,596
#102
1
199,976
399,959
599,946
799,921
999,907
1,199,891
1,399,880
1,599,865
1,799,847
1,999,825
2,307,179